Environ Monit Assess (2024) 196:277
https://doi.org/10.1007/s10661-024-12342-6

REVIEW

UAV and satellite remote sensing for inland water quality assessments: a literature review

Eden T. Wasehun · Leila Hashemi Beni · Courtney A. Di Vittorio

Received: 1 August 2023 / Accepted: 8 January 2024 / Published online: 17 February 2024

Abstract High spatial and temporal resolution data is crucial to comprehend the dynamics of water quality fully, support informed decision-making, and allow efficient management and protection of water resources. Traditional in situ water quality measurement techniques are both time-consuming and labor-intensive, resulting in databases with limited spatial and temporal frequency. To address these challenges, satellite-driven water quality assessment has emerged as an efficient and effective solution, offering comprehensive data on larger-scale water bodies. Numerous studies have utilized multispectral and hyperspectral remote sensing data from various sensors to assess water quality, yielding promising results. However, the recent popularity of unmanned aerial vehicle (UAV) remote sensing can be attributed to its high spatial and temporal resolution, flexibility, ability to capture data at different times of day, and relatively low cost compared to traditional platforms. This study presents a comprehensive review of the current state of the art in monitoring water quality in small inland water bodies using satellite and UAV remote sensing data. It encompasses an overview of atmospheric correction algorithms and the assessment of different water quality parameters. Furthermore, the review addresses the challenges associated with monitoring water quality in these bodies of water and emphasizes the potential of UAVs to overcome these challenges by providing accurate and reliable data.

Keywords Water quality · High resolution · Satellite images · UAV · Multispectral · Hyperspectral

E.T. Wasehun
Applied Science and Technology, North Carolina A&T State University, 1601 E Market St, Greensboro, NC 27411, USA
e-mail: etwasehun@aggies.ncat.edu

L. Hashemi Beni (✉)
Department of Build Environment, North Carolina A&T State University, 1601 E Market St, Greensboro, NC 27411, USA
e-mail: lhashemibeni@ncat.edu

C. A. Di Vittorio
Department of Engineering, Wake Forest University, 1834 Wake Forest Rd, Winston-Salem, NC 27109, USA
e-mail: divittoc@wfu.edu

Introduction

Water, particularly inland water bodies, plays a crucial role in various sectors such as agriculture, urban planning, industry, aquaculture, recreation, wildlife, and ecological health (Wang et al., 2022; Welcomme, 2011). With the rapid growth of the global population, the increased demand for water access and use has caused increased pollution and degraded water quality (United Nations, 2022). Water quality impairments can occur due to elevated nutrient levels, resulting from the discharge of pollutants in residential and industrial areas (Karakoc et al., 2003; Osibanjo et al., 2013), excessive use of fertilizers and pesticides (Dosskey, 2001; Muscutt et al., 1993), changes in land use/land cover (El Saadi et al., 2014; Mbuh, 2019; Rostom et al., 2017), and erosion during storm events (Grissinger & McDowell, 1970). Given the potential impact of poor water quality on both human health and marine ecosystems, the assessment of water quality holds utmost significance. Hence, it is essential to employ effective methods for measuring water quality to ensure sustainable management. Regular and extensive assessments are necessary for the adaptive management of water bodies, facilitating the development of long-term plans and the implementation of new policies and regulations based on the intricate relationships between human practices and water quality within lakes and reservoirs (United Nations Environment Programme, 2021).

Water quality parameters encompass the physical, chemical, and biological characteristics of a water body (Gholizadeh et al., 2016; Wen & Yang, 2011). Traditionally, these parameters are measured from small volumes of water using in situ sensors or grab samples that are subsequently analyzed in a laboratory. However, it is important to note that water quality exhibits spatial-temporal variability across the water surface (Sagan et al., 2020). Spatial variability refers to variations in parameter values or concentrations across different locations, while temporal variations represent changes caused by seasonal fluctuations in natural processes, such as temperature, precipitation, and hydrological conditions (Zhang et al., 2008). Consequently, attempting to discern water quality using limited samples poses challenges, necessitating thorough sampling and measurement. The use of traditional techniques in this regard can be expensive, labor-intensive, and time-consuming, and collecting a sufficient number of samples to adequately represent an entire water body is often impractical. These limitations impede the attainment of continuous and synoptic water quality assessments (Giardino et al., 2001; Nas et al., 2009; Skarbøvik & Roseth, 2014).

Remotely sensed water quality assessment presents a promising approach to overcome the limitations of traditional methods and enables more cost-effective, efficient, and larger-scale monitoring and assessments. In recent years, unmanned aerial vehicles (UAVs) have gained popularity for remote water quality assessment due to their ability to provide very high spatial and temporal resolution data. This capability is particularly valuable for monitoring small inland water bodies such as lakes, streams, rivers, wetlands, or reservoirs (Castro et al., 2020; Cui et al., 2022; Govender et al., 2007; Guimarães et al., 2019; Isgró et al., 2022; Keith et al., 2014; Moses et al., 2015; Murugan et al., 2016; Olivetti et al., 2020; Su et al., 2015; Tan et al., 2011; Wu et al., 2014; Yang et al., 2022; Zang et al., 2012; Zeng et al., 2017; Zhang et al., 2023, 2021).

While several reviews have explored water quality assessment with a focus on utilizing multi-sourcing and multi-sensor satellite remote sensing data (Gholizadeh et al., 2016; Palmer et al., 2015; Yan et al., 2015; Yang et al., 2022), there is a literature gap regarding the joint review of UAV and satellite remote sensing of water quality in small inland water bodies. A comprehensive review is needed to support managers in evaluating trade-offs and selecting the most appropriate measurement technique. As a result, this study aims to bridge this gap in the literature by reviewing the current state-of-the-art water quality monitoring using both satellite and UAV remote sensing data for small inland water bodies. The review encompasses an analysis of the challenges associated with monitoring water quality in such water bodies using satellite remote sensing data, as well as the potential of UAVs to overcome these challenges and provide reliable data.

Remote sensing for water quality assessments

Remote sensing data plays a vital role in studying the Earth's surface, examining changes, identifying problems, and formulating solutions for maintaining or enhancing the environment. Advancements in technology have contributed to the widespread use of remote sensing data in water quality assessments, yielding promising and satisfactory results (Guimarães et al., 2019; Olivetti et al., 2020; Zhang et al., 2023). This approach provides data across various spatial and temporal scales in a cost-effective and time-efficient manner (Mbuh, 2019). Moreover, the automatic and continuous acquisition of data allows for the timely identification of surface changes on Earth (Chebud et al., 2012). To date, numerous studies have leveraged remote sensing data for diverse applications, including water volume calculations (Lu et al., 2013), water resource management (Giardino et al., 2010), groundwater mapping (Elbeih, 2015), water bodies identification (Sun et al., 2012), water storage and level measurements (Frappart, 2005), and water quality monitoring in both small and large water bodies (Bresciani et al., 2017; Castro et al., 2020).

Remote sensing has been proven to be a valuable and effective method for capturing water quality parameters (Bonansea et al., 2018; Hellweger et al., 2004; Saberioon et al., 2020; Su & Lo, 2022; Yulong et al., 2022). Various water quality components are developed and used to determine the presence and level of contamination using remote sensing, thus asserting water quality. These components are measured based on their reflectance signals, known as water-leaving radiance, captured by the sensors. Figure 1 displays the interaction of light between water quality components and sensors. The reflectance, absorbance, and scattering spectral characteristics of these components, called inherent optical properties (IOP) (IOCCG, 2006), make it possible to detect and monitor water pollutants using spectral reflectance signatures (Rostom et al., 2017; Wen & Yang, 2011). Optically active components can be directly measured using the relationship between inherent optical properties (IOP) and remote sensing reflection (Kirk, 1994; Kutser, 2004; Matthews, 2011). In contrast, optically inactive components do not exhibit optical activity and do not interact with light in the same way as optically active parameters. Due to the low optical properties and low signal-to-noise ratio of optical inactive components (Gholizadeh et al., 2016; Yang et al., 2022), several studies have primarily focused on optically active components. Similarly, the optically active properties are often used as proxies to estimate optically inactive properties (Yang et al., 2022). Table 1 presents commonly measured water quality parameters using remote sensing techniques.

Platforms and sensor types

Water quality components can be assessed using multispectral and hyperspectral optical sensors deployed on both airborne and satellite platforms (Fig. 2). Each of these platforms and sensor types is described next in the context of inland water quality monitoring.

Satellite platform

Satellite platforms have transformed water quality assessments by providing a broad-scale and comprehensive view of water bodies on the Earth's surface. These platforms have the advantage of enabling continuous monitoring of large areas without causing any disturbance to the aquatic environment. This feature makes satellite-based platforms an invaluable tool for environmental assessment and management (Harvey et al., 2015; Topp et al., 2020).

UAVs platform

Unmanned aerial vehicles/systems (UAVs/UASs), commonly known as drones, have emerged as an effective remote sensing platform for environment monitoring (Cheng et al., 2020; Gebrehiwot & Hashemi-Beni, 2021; Hashemi-Beni & Gebrehiwot, 2021). UAVs offer several advantages over satellite remote sensing, such as the ability to fly at lower altitudes (Castro et al., 2020; Olivetti et al., 2020), providing higher spatial resolution, and offering flexible deployment options at a reasonable cost (Isgró et al., 2022).

Multispectral sensors

Multispectral sensors capture data within a limited number of bands, typically ranging from 5 to 10 bands with broad spectral resolution. These bands cover wavelengths from 430 to 1500 nm, encompassing the visible, near-infrared, and short-wave infrared regions of the electromagnetic spectrum. Multispectral sensors have been extensively employed for the detection and monitoring of water body dynamics and quality (Bonansea et al., 2018; Castro et al., 2020; He et al., 2008; Hellweger et al., 2004; Knight & Voth, 2012; Pahlevan et al., 2020; Soriano-González et al., 2022).

Hyperspectral sensors

Hyperspectral sensors capture several narrow and continuous spectral bands across the entire spectrum, from visible to thermal infrared regions. These sensors can record hundreds of spectral bands in a single acquisition (Govender et al., 2007), providing detailed spectral information for each pixel in an image. As a result, hyperspectral remote sensing data offers exceptional differentiation of water quality parameters based on their narrow-band spectral response. Its capability to capture fine-grained spectral information and identify specific water quality parameters has made hyperspectral data particularly valuable for monitoring and characterizing water quality parameters (Banerjee & Shanmugam, 2021; Giardino et al., 2007; Östlund et al., 2001; Palmer et al., 2015; Zeng et al., 2017).

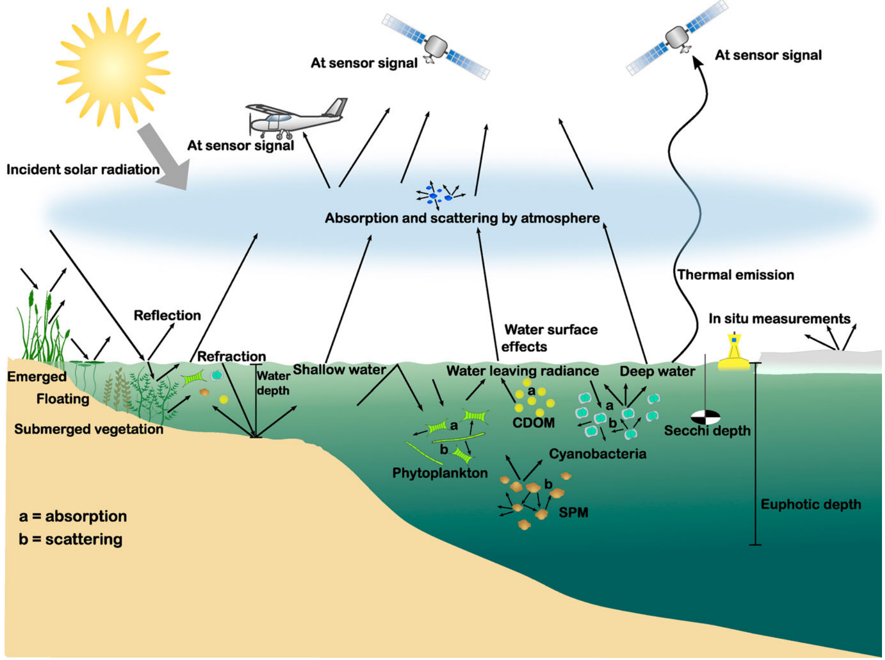

Fig. 1 Interactions of light between water quality components and sensors (Dörnhöfer & Oppelt, 2016)

In certain investigations, researchers have employed a combination of multispectral and hyperspectral sensors to obtain comprehensive data sets, resulting in cost-effective solutions (Giardino et al., 2010; Topp et al., 2020; Yang et al., 2022). Similarly, in ongoing efforts to maximize the periodicity of data acquisition and address data gaps in small inland water bodies, several studies have applied a combination of satellite and UAV platforms. These studies conduct separate analyses and develop predictive models (Castro et al., 2020). Additionally, other studies focus on integrating and fusing the datasets to construct predictive models (Rahul et al., 2023). This approach aims to enhance the accuracy of inland water quality monitoring by leveraging the unique strengths of both satellite and UAV technologies. Tables 2 and 3 provide an overview of commonly used satellite and UAV sensors, including their spectral and spatial resolutions.

Data pre- and postprocessing

Preprocessing

The preprocessing of remote sensing data is a crucial step in obtaining accurate information and improving the retrieval of water quality parameters. This process involves multiple steps, including geometric correction (Nas et al., 2009), radiometric correction, and primarily atmospheric correction. Each of these steps plays a significant role in ensuring the quality and accuracy of the data. Geometric correction involves aligning and georeferencing the remote sensing data to ensure precise spatial alignment. This step is essential for accurate analysis and comparison of different datasets. Radiometric correction is the process of calibrating the sensor data to convert digital numbers into physical units of radiance or reflectance. By removing sensor-specific effects and calibrating the data, radiometric correction allows for quantitative analyses and comparisons of images acquired at different times or by different sensors.

Atmospheric correction is a critical preprocessing method that corrects the influence of atmospheric components on the remote sensing data. Atmospheric effects, such as aerosols, water vapor, and atmospheric path radiance, can significantly impact the accuracy of the data, especially in aquatic environments. The successful application of remote sensing algorithms for water quality assessment relies on employing appropriate atmospheric correction methods to accurately retrieve the remote sensing reflectance (Hu et al., 2004; Hussein & Assaf, 2020; Moses et al., 2017). This correction is particularly important in mitigating the atmo-

Table 1 Commonly measured water quality parameters

Optical property	Water quality parameter	Abbreviation
Optically active	Chlorophyll-a	Chl-a
	Total suspended matter/solid/sediment	TSM/TSS
	Turbidity	TUR
	Chromophoric/colored dissolved organic matter	CDOM
	Secchi disk depth/Secchi disk transparency	SDD/SDT
	Total dissolved solids	TDS
	Electrical conductivity/specific conductance	EC/ SC
	Temperature	T^0
	Crude oil contamination	C.O
	Fluorescent dissolved organic matter	fDOM
	Salinity	S
	Phycocyanin (characteristic pigment of cyanobacteria)	PC
Optically inactive	pH	pH
	Biological oxygen demand/biochemical oxygen demand	BOD
	Chemical oxygen demand	COD
	High dissolved oxygen	HDO, DO
	Oxygen	O_2
	Dissolved organic carbon	DOC
	Particulate organic carbon	POC
	Phosphorus/total phosphorus/dissolved phosphorus	P
	Ortho-phosphate	PO_4
	Oxidation-reduction potential	ORP
	Nitrogen	N
	Ammonia nitrogen	NH3-N
	Nitrate nitrogen	NO3-N
	Potassium permanganate oxidant	COD_{Mn}
	Total alkalinity	TA

spheric effects on water bodies, which typically exhibit low reflectance values (Martins et al., 2017; Pahlevan et al., 2021). The specific preprocessing methods required may vary depending on the type of remote sensing data, platforms, and water type (Pahlevan et al., 2021).

Satellite remote sensing

Satellite data often requires more rigorous atmospheric correction than UAV data due to the higher altitude and greater atmospheric attenuation. Several atmospheric correction algorithms have been designed for aquatic environments to obtain reliable water-leaving radiance estimates from satellite measurements. In brief, these algorithms can be categorized into two groups: image-based models and radiative transfer codes models (RTCs) (Hadjimitsis et al., 2004). The first group, image-based atmospheric correction techniques, utilizes the information contained within the satellite image itself to estimate and correct atmospheric effects. These methods employ look-up tables to simulate the interaction of radiation with the atmosphere based on the estimated aerosol optical thickness (Mobley et al., 2016). Some commonly used algorithms in this category include atmospheric correction for L8 OLI and Sentinel 3 Ocean and Land Colour Instrument (ACOLITE) (Ansper & Alikas, 2018; Page et al., 2019; Pahlevan et al., 2020; Rodrigues et al., 2017; Saberioon et al., 2020), Case 2 Regional Coast Colour processor (C2RCC) (Ansper & Alikas, 2018; Isgró et al., 2022; Shen et al., 2020), Improved Contrast between Ocean

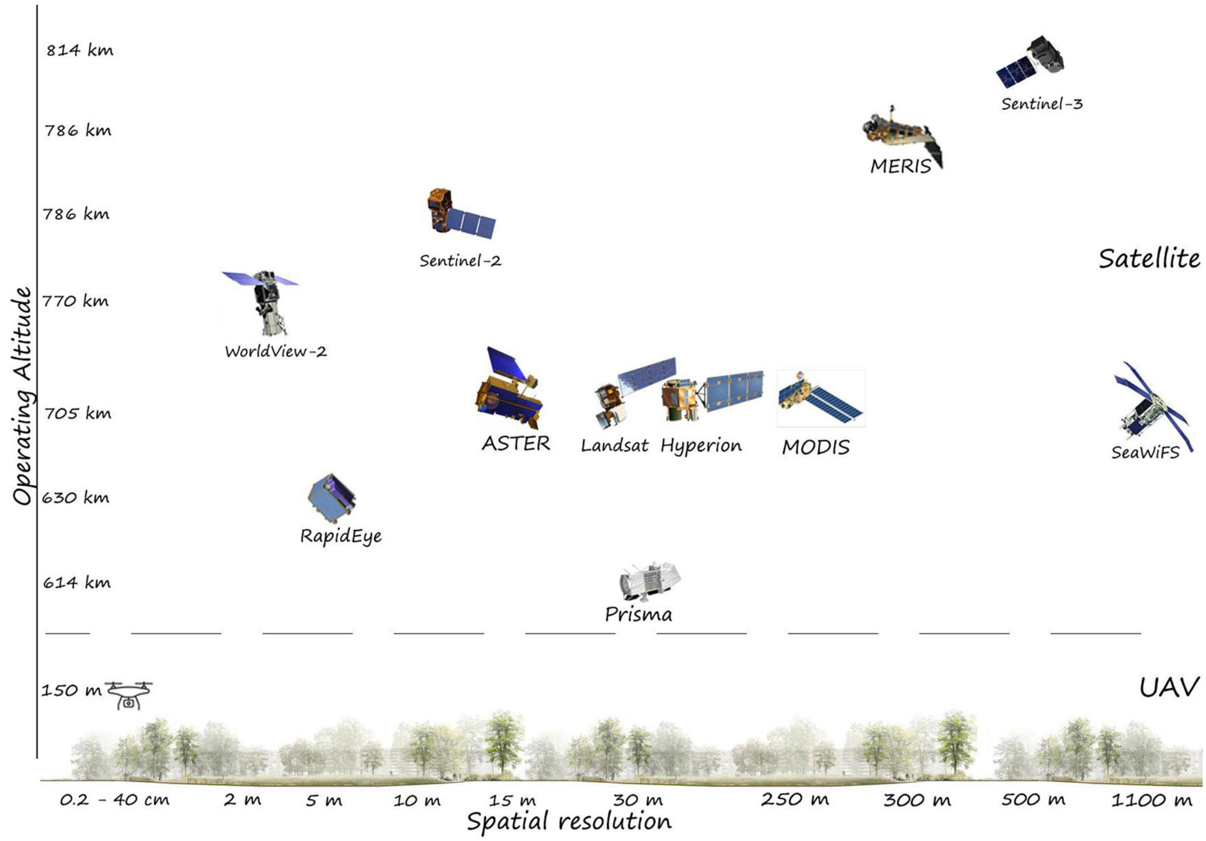

Fig. 2 Remote sensing platforms operating altitudes and spatial resolution

and Land (ICOL) (Bresciani et al., 2017; Harvey et al., 2015; Philipson et al., 2016), POLYnomial-based algorithm applied to MERIS (POLYMER) (Ansper & Alikas, 2018; Pahlevan et al., 2020; Shen et al., 2020), and SeaWiFS Data Analysis System (SeaDAS) (Banerjee & Shanmugam, 2021; Chavula et al., 2009; Dev et al., 2022; Pahlevan et al., 2021, 2020; Shen et al., 2020). These algorithms are relatively simple to implement and require minimal ancillary data, making them accessible to a wide range of users and applications. However, they may encounter limitations in complex atmospheric conditions or when dealing with specific optical properties of water bodies (Ansper & Alikas, 2018; Rodrigues et al., 2017).

The second group, radiative transfer code (RTC) models, simulates the interaction of solar radiation with the atmosphere and the underlying surface. These models take into account atmospheric constituents, such as gases, aerosols, clouds, and profiles (e.g., temperature, pressure, humidity), as well as surface properties (e.g., reflectance, emissivity) and sensor characteristics to quantify the atmospheric effects on satellite measurements (Vermote et al., 1997). The most commonly used RTC models for inland and coastal waters are quasi-analytical algorithm (QAA) (Li et al., 2016; Ogashawara et al., 2022) and generalized IOP algorithm (GIOP) (Shi & Wang, 2019; Werdell et al., 2013). RTC-based algorithms provide physically meaningful surface reflectance values, allowing for quantitative analysis and accurate comparison of remote sensing data. However, they require accurate estimation of atmospheric parameters and input data, and uncertainties in these parameters can introduce errors in the correction process (Kutser, 2012).

In addition to water-specific atmospheric correction models, several researchers have also utilized atmospheric correction algorithms designed for land environments. The dark object subtraction (DOS) algorithm

Table 2 Commonly used satellite-based sensor for water quality assessment

Sensor	Type	Name	Duration	Spectral resolution (nm)	Spatial resolution (m)	Revisit day
Multispectral	Low resolution	Sea-viewing Wide Field-of-view Sensor (SeaWiFS)	1 August 1997 – 11 December 2012	8 bands (402–885) VNIR	1100	1–2
		Moderate Resolution Imaging Spectroradiometer (MODIS)	18 December 1999–present	36 bands (405–2155) 1–19 (3660–14,280) 20–36	250–1000	1–2
		Medium Resolution Imaging Spectrometer (MERIS)	March 2002–8 April 2012	15 bands (390–1040) VNIR	300	3
		Sentinel-3 Ocean and Land Color Instrument (OLCI)	16 February 2016–present	21 bands (400–1020) VNIR	500	27
	Medium resolution	Landsat TM	March 1984–5 June 2013	7 bands (450–1750 nm) VNIR, (1040–1250 nm) thermal, (2080–2350 nm) mid-infrared	30–120	16
		Landsat-7 ETM +	6 April 2022–present	8 bands (450–900 nm) VIR, (1500–1750 nm) SWIR, (1040–1250 nm) thermal, (2080–2350 nm) mid-infrared, (520–90) nm PAN	30-60-15	16
		Landsat-8 OLI/TIRS and Landsat-9 OLI-2	February 2013 (for OLI) and 27 September 2021 (for OLI-2)–present	11 bands (430–880) VNIR, (500–680) Pan, (1570–2290) 2SWIR, (1360–1380) Cirrus, (10,600-12,510) 2TIRS	30-15-100	16
	High resolution	Advanced Spaceborne Thermal Emission and Reflection Radiometer (ASTER)	18 December 1999–present	14 bands (520–860) VNIR (1600–2430) SWIR, (8125–11,650) TIR	15-30-90	16

Table 2 continued

Sensor	Type	Name	Duration	Spectral resolution (nm)	Spatial resolution (m)	Revisit day
		Sentinel 2 MSI	23 June 2015–present	12 bands (443–665) VIS, (842) NIR, (705–783) 3Vegetation Red Edge, (1375–2190) 3SWIR	10-20-60	10
		RapidEye	29 August 2008–31 March 2020	5 bands (440–850) VNIR	5	1
		WorldView-2	8 October 2009–present	8 bands (450–800nm) VNIR	2	1.1
Hyperspectral	Low resolution	Hyperspectral Imager for The Coastal Ocean (HICO)	10 September 2009–13 September 2014	128 bands (353–1080 nm), 5.7 nm bandwidth	90	3
	Medium resolution	Advanced Hyper Spectral Imager (AHSI)	12 September 2019–present	166 bands (400–2500), 76 in VNIR, and 90 in SWIR 10 and 20 nm bandwidth	30	3
		Hyperion	23 November 2000–30 March 2017	220 bands (400 to 2500 nm) VNIR to SWIR, 10 nm bandwidth	30	16
		Prisma	22 March 2019–present	239 bands (400–2500 nm), 66 VNIR (400–1010 nm) and 173 SWIR (920–2500 nm), and panchromatic (400–700 nm), ¡12 nm bandwidth	30–5	29
		HawkEye Ocean Color Imager	3 December 2018–present	400 to 1000	30	9

Table 3 Commonly used UAV-based sensors for water quality assessment

Type	Sensor	Number of bands	Spectral resolution (nm)	Spatial resolution (cm)
Multispectral	RedEdge Micasense	5 bands (475–840 nm) VNIR	B and G 20, R and red-edge 10 and NIR 40	8
	MicaSense RedEdge-MX Dual	10 bands (444–842 nm) VNIR	–	8
	Canon Powershot S110 RGB and NIR sensors	3 RGB bands (450–660 nm) and 3 NIR bands (550–850nm)	–	3.5
	Canon ELPH 110HS camera	3 NGB bands (NIR, green, and blue)	–	5
	DJI Phantom 4	3 RGB bands (400–700 nm)	–	3.1
	Parrot Sequoia	4 bands (550–790) green - NIR	40	13
Hyperspectral	Gaia Sky-M	272 bands (399.69–1001.08 nm)	2.21	0.2
	Headwall NANO-Hyperspec	270 bands (400–1000 nm)	6	17.3
	Gaiasky-mini2-VN	176 bands (400–1000 nm)	4	27
	Gaia Sky-mini	270 bands (401.81–999.28 nm)	–	40

is widely used in water quality monitoring (Bonansea et al., 2015; Carvalho et al., 2022; Markogianni et al., 2020; Matthews et al., 2010; Zhou et al., 2008). It assumes that certain dark targets in an image, such as deep-water bodies or dark pixels, exhibit no atmospheric signal and can serve as references for atmospheric correction. Other atmospheric correction algorithms, such as Sen2cor atmospheric correction procedure for MSI imagery (Ansper & Alikas, 2018; Grendaitė et al., 2018; Kutser et al., 2016; Toming et al., 2016; Yang et al., 2022), atmospheric and topographic correction method (ATCOR) (Bresciani et al., 2019; Chebud et al., 2012; Kutser et al., 2016; Rodrigues et al., 2017), Land Surface Reflectance Code (LaSRC) (Peterson et al., 2020; Rubin et al., 2021), Second Simulation of a Satellite Signal in the Solar Spectrum (6 S) (Bonansea et al., 2015; Bresciani et al., 2017; Flores-Anderson et al., 2020; Ma & Dai, 2007; Matthews et al., 2010; Oyama et al., 2009; Shen et al., 2020), and Fast Line-of-Sight Atmospheric Analysis of Hypercubes (FLAASH) (Abdelmalik, 2018; Ha et al., 2017; Kutser, 2012; Kutser et al., 2005; Rodrigues et al., 2017; Tebbs et al., 2013; Watanabe et al., 2015; Yang et al., 2022) have been applied for different types of satellite imagery.

UAV remote sensing

One significant advantage of UAV remote sensing is that the imagery captured by UAVs is less affected by atmospheric conditions compared to satellite imagery (Castro et al., 2020; Del Pozo et al., 2014; Zeng et al., 2017). Since UAVs fly at lower altitudes, the atmospheric effects on the imagery are minimized, but rather, the acquired imagery may suffer from more distortions and perspective effects (Zang et al., 2012). Because of this, in UAV remote sensing, more attention is typically given to geometric correction to rectify these distortions and align the UAV imagery accurately (Su et al., 2015). Additionally, other preprocessing steps, such as georeferencing, reflectance correction, and ortho-mosaicking, are necessary for UAV imagery (Castro et al., 2020; Cheng et al., 2020; Guimarães et al., 2017; Isgró et al., 2022; Olivetti et al., 2020; Zhang et al., 2021, 2020).

Data analysis

Coastal and inland water bodies are often characterized as Case II and exhibit complex optical properties due to the presence and varying concentrations of organic matter, suspended particles, and dissolved substances (Doerffer et al., 1999; Morel & Prieur, 1977). For example, chlorophyll-a, a pigment utilized in photosynthesis by plants and algae, shows high reflectance in the green (reflectance peak at 550 nm), red-edge (670–675 nm), and near-infrared (reflectance peak at 700 nm) spectral bands, as well as high absorption in the blue (450–475 nm) spectral range (Avdan et al., 2019; Castro et al., 2020; Gholizadeh et al., 2016; Hussein & Assaf, 2020; Zhang et al., 2022). On the other hand, suspended particles, which consist of sediment, organic matter, and plankton (containing algal cells) suspended in the water column, are characterized by high reflectance throughout the spectral range, while colored dissolved organic matter (CDOM) absorption increases with decreasing wavelength, from blue to some portion of the green. Figure 3 shows the spectral characteristics of water with high turbidity, chlorophyll-a, and colored dissolved organic matter. Complex waters can contain all three constituents, introducing complexity in the relationship between the sensor radiance and the water quality parameters (Sudheer et al., 2006) and posing challenges for remote sensing-based water quality retrieval (Maciel et al., 2021). To overcome these challenges, specific retrieval algorithms that account for the unique spectral responses of the constituents are needed (Harvey et al., 2015; Yang et al., 2022). Indeed, numerous models, such as those implemented in the NASA SeaDAS software (https://seadas.gsfc.nasa.gov), have been developed on global and larger regional scales. However, these models may not be suitable for most inland water bodies since they were originally designed for Case I water bodies, such as oceans, characterized by a dominant presence of chlorophyll-a. These models often rely on simpler algorithms that may not adequately capture the complexity of inland water systems (Qin et al., 2007). As a result, developing models for inland water bodies necessitates a high degree of customization, tailoring them to the specific characteristics of the inland water, including its unique properties and water type. Unlike open oceans, inland water ecosystems exhibit diverse dynamics, requiring more meticulous and context-specific approaches to achieve accurate predictions of water quality. Developing and utilizing these algorithms are essential for effective water quality monitoring and management in complex aquatic environments.

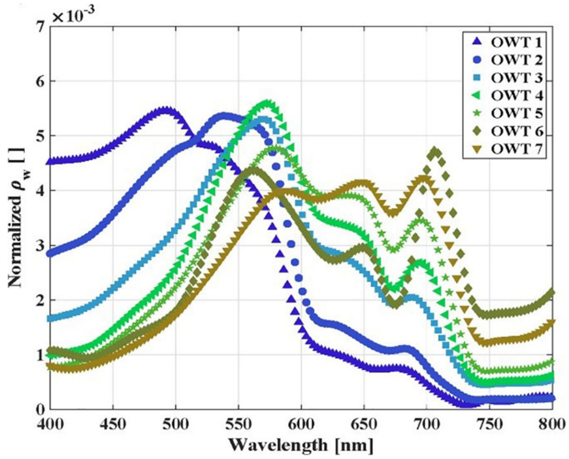

Fig. 3 Spectral illustration of water with high turbidity, chlorophyll-a (Chl-a), and colored dissolved organic matter (CDOM) (Pahlevan et al., 2021). OWT stands for optical water types, a classification based on water's reflectance and absorption. OWT1 and OWT2 represent clear waters, OWT3 shows high chlorophyll concentrations, OWT4, OWT5, and OWT6 indicate high concentrations of different phytoplankton blooms and high turbidity, and OWT7 represents waters with high sediment concentrations

To address the difficulties associated with monitoring Case II waters, various approaches have been developed and used for the accurate retrieval of water constituent concentrations from remote sensing data. Figure 4 shows a framework acquisition and analysis of water quality parameters using remote sensing data. In this review, these approaches are categorized as follows: empirical methods, semi-analytical methods, and artificial intelligence (AI) approaches.

Empirical approach

The empirical approach establishes statistical relationships between remote sensing observations and water quality parameters. This approach can involve single band analysis (Brezonik et al., 2009; El Saadi et al., 2014; Simis et al., 2005; Tarrant et al., 2010), band combinations including ratio (He et al., 2008; Kutser et al., 2005), or band indices (Castro et al., 2020). The relationships can be expressed as linear functions (Toming et al., 2016), power functions (Ha et al., 2017), or polynomial functions (Flores-Anderson et al., 2020), depending on the regression analysis and the dynamic range of the calibration data used (Yang et al., 2011). The empirical approach is simple, flexible, and relatively easy to implement (Matthews et al., 2010). However, the physical interpretability of models is limited, as they do not explicitly incorporate underlying physi-

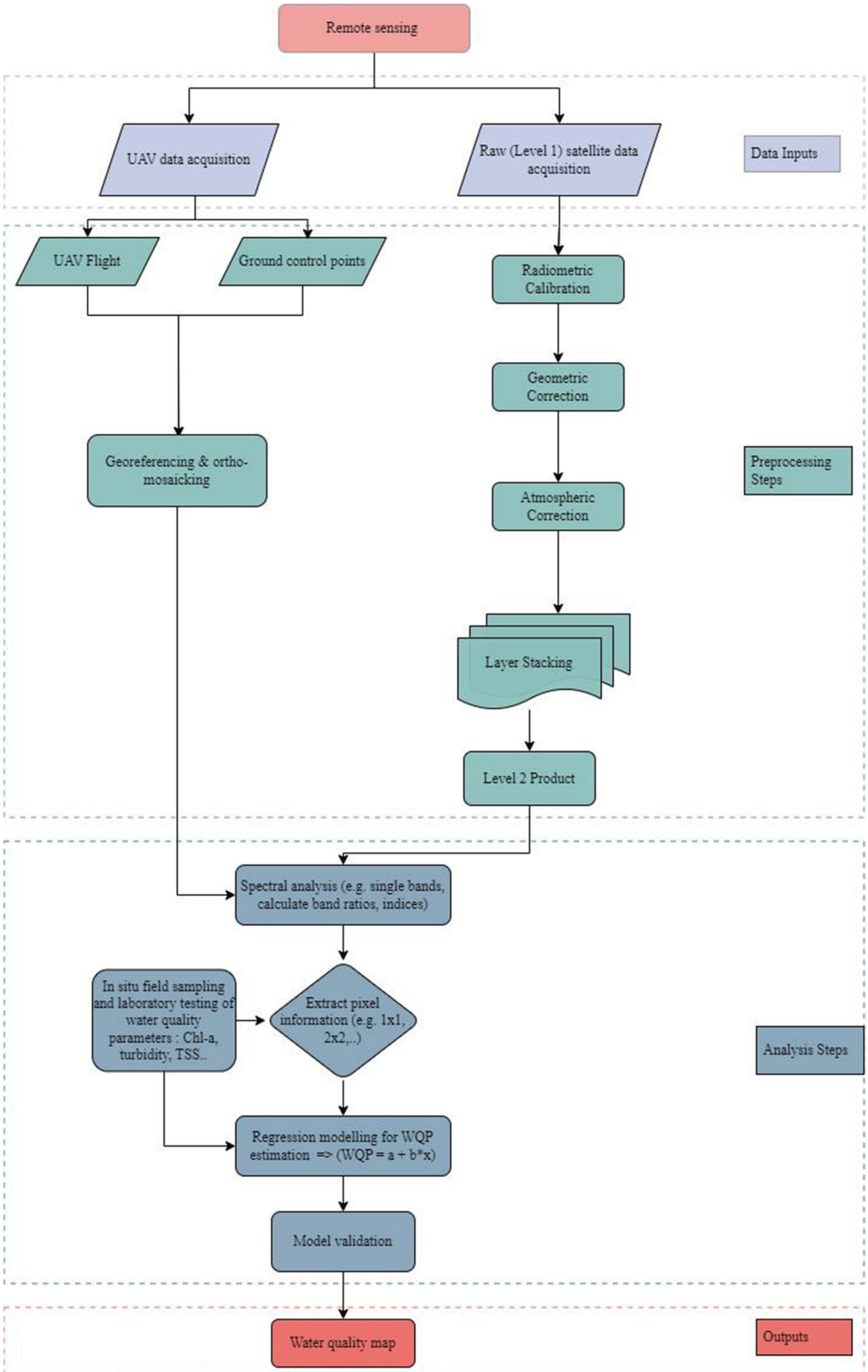

Fig. 4 Workflow for water quality parameters prediction using remote sensing data

cal processes, making it difficult to derive mechanistic insights. Transferability and generalization of empirical models can also be challenging when applied to different regions or time periods due to variations in water body composition and optical properties (Bukata, 2005; Fukushima et al., 2016; Oyama et al., 2009). Likewise, empirical models heavily rely on the availability of accurate and representative ground truth data, which can be limited or expensive to acquire.

Semi-analytical approach

The semi-analytical approach combines physical principles, such as radiative transfer models and bio-optical algorithms, along with empirical relationships to retrieve water quality information from remote sensing data. This approach provides a more mechanistic understanding of the underlying processes (Lee et al., 2015). Retrieving inherent optical properties allows for improved atmospheric correction, improving water quality parameter estimation accuracy. The semi-analytical approach can capture complex bio-optical relationships, making it applicable to various aquatic environments (Mishra et al., 2014). However, it requires accurate and representative input parameters, including accurate atmospheric correction and knowledge of inherent optical properties (Matthews et al., 2010). Representing the complexity of bio-optical processes and the variability of environmental conditions also poses challenges in modeling (Yang et al., 2011). Calibration and validation can be difficult, particularly when ground truth data are limited or hard to obtain (Yang et al., 2011).

Artificial intelligence techniques

The emergence of AI techniques has revolutionized water quality monitoring from remote sensing data. These data-driven techniques can handle large volumes of data and extract complex patterns without prior knowledge that may not be evident to traditional approaches (Chang & Vannah, 2013; Keller et al., 2018), and capture nonlinear relationships between remote sensing variables and water quality parameters (Maciel et al., 2021; Rubin et al., 2021; Sudheer et al., 2006). They can adapt to changing environmental conditions and integrate multi-source and multi-sensor data (Chang & Vannah, 2013), resulting in improved estimation accuracy (Sudheer et al., 2006). AI models enable automation and efficiency of water quality monitoring processes. Support vector regression (SVR), artificial neural network (ANN), and extreme gradient boosting (XGBoost) are commonly used AI models in water quality retrieval, and they have shown great success and relatively satisfactory results in many recent studies (Arias-Rodriguez et al., 2021; Hafeez et al., 2019; Tian et al., 2023; Xiao et al., 2022; Yan et al., 2023). Figure 5 illustrates a neural network structure for water quality retrieval. Although most studies using AI approaches have reported significant results, there are limitations to consider. Large and representative training datasets are required to effectively train AI models. Insufficient or biased training data may lead to poor generalization and inaccurate predictions. The black-box nature of some AI algorithms limits their interpretability, hindering the understanding of underlying processes (Petch et al., 2022). Overfitting can occur if models are overly complex or trained on limited datasets, compromising their performance on new data. Moreover, implementing AI approaches requires computational resources and expertise for model development, implementation, and maintenance.

Satellite remote sensing

Multispectral remote sensing

A number of multispectral satellite sensors have been used for quantitative monitoring of water quality parameters. All the images are free of charge, publicly available, and provided in single and multi-day aggregate products in a variety of spatial and spectral resolutions.

Among the several multispectral satellite sensors specifically designed for ocean color measurements, Sentinel-3 Ocean and Land Color Instrument (OLCI), Medium Resolution Imaging Spectrometer (MERIS), Coastal Zone Color Scanner (CZCS), Moderate Resolution Imaging Spectroradiometer (MODIS), and Sea-viewing Wide Field-of-view Sensor (SeaWiFS) have been widely used in inland water quality monitoring. These sensors offer advantages such as repeat cycles (e.g., 1–2 days), narrow spectral bands (ranging from 400 to 1100 nm), and high radiometric resolution. However, their spatial resolution (respectively of the order of 300 m to 1.1 km) is limited to large-scale water monitoring, such as an open ocean, where chlorophyll-a is the major optically active constituent. Inland water bodies with complex optical characteristics may experience reduced estimation precision, which can hinder the monitoring of water quality changes, particularly

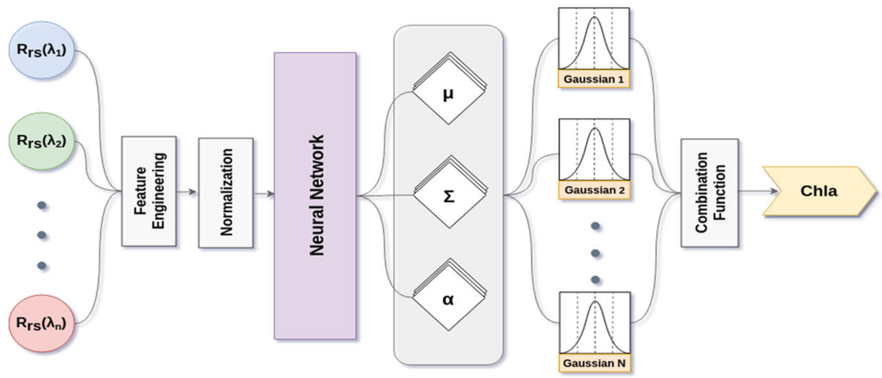

Fig. 5 Illustration of neural network for chlorophyll-a retrieval (Pahlevan et al., 2020)

at specific sites of interest (Topp et al., 2020). Some of the models for water quality parameters are listed in Table 4.

There are several satellites that have sufficient spatial resolution for use in inland water quality monitoring studies. These include the Landsat program (including Landsat's Thematic Mapper (TM), Enhanced Thematic Mapper Plus (ETM+) and Operational Land Imager (OLI)), Sentinel-2, Advanced Spaceborne Thermal Emission and Reflection Radiometer (ASTER), WorldView, and Satellite Pour I'Observation de la Terre (SPOT). Despite these sensors being primarily designed for land-based remote sensing applications and having less frequent satellite revisit time (3–16 days vs. 1 daily revisit for ocean color sensors), several studies have estimated and proposed reliable algorithms between the remote sensing data and water quality parameters in inland water. Examples of parameters studied include chlorophyll-a (Cao et al., 2020; Chebud et al., 2012; Lu et al., 2021; Sudheer et al., 2006), water clarity (Maciel et al., 2021; Shen et al., 2020), and total suspended sediments (Sudheer et al., 2006). The patterns observed in these satellite sensors demonstrate more detail than those of the water-based sensors due to the resolution of 10–30 m as opposed to 300 m respectively. Some of the models for water quality parameters using land-based sensors are presented in Table 5.

Although multispectral satellites provide data in different spectral bands, the number of bands and their specific wavelengths may not be optimized for water quality monitoring (Fu et al., 2018). Some water quality parameters, such as chlorophyll-a concentration, as shown in Tables 4 and 5, are typically measured using visible NIR bands, and their spectral ranges may overlap with other optically active water quality parameters. This overlap can lead to challenges in accurately estimating these parameters using multispectral satellite data. Certain water quality parameters, such as suspended particle matter and turbidity, have shown higher correlations with specific spectral combinations (Avdan et al., 2019), emphasizing the need for more specific spectral bands or higher spectral resolution than what is available in multispectral satellite data.

Researchers (Dekker et al., 2001; Gholizadeh et al., 2016; Ha et al., 2017; Kutser et al., 2016) have highlighted that the distribution of spectral bands in most multispectral satellite sensors, such as Landsat-7 ETM+, Landsat 8 OLI, Sentinel-2, ASTER, and SPOT HRV, further complicates the extraction of exact reflectance and absorbance peak points for each water quality parameter. The spectral band positioning of Landsat-7 ETM + and Landsat 8 OLI with respect to spectral characteristics of water quality parameters are presented in Fig. 6. This limitation can indirectly result in the overlapping of reflectance signature positions and omission of reflectance peak for certain parameters, leading to errors in their estimation.

Hyperspectral remote sensing

The fine spectral resolution of hyperspectral satellite sensors allows for more precise and accurate identification and quantification of specific absorption and reflectance of certain water quality parameters, thus reducing the issue of parameter overlapping that commonly occurs in multispectral data. Additionally, it facilitates the development of advanced retrieval algorithms specifically tailored to estimating water quality parameters. These algorithms can exploit detailed spectral information to derive more precise relationships between spectral signatures and the corresponding water quality measurements. This leads to improved accuracy in estimating parameters such as

Table 4 Retrieval models using low spatial resolution satellite multispectral data

Sensor	Method	Parameter(s)	Temporal observation	Band/equation	Training Acc	Validation Acc	Ref
MERIS	EM	PC	April–Sep 2003	$Singleband: Rrs(620)$	$R^2: 0.97$	–	Simis et al. (2005)
MERIS	EM	Chl-a	August 14th, 2003	$Bandratio: \frac{Rrs(412.5)}{Rrs(665)}$	$R^2: 0.81$	–	Gons et al. (2008)
MERIS	DL	Chl-a	April to September 2008 and 2010	Free University Berlin (FUB)	r: 0.9	–	Harvey et al. (2015)
MERIS	SA	Chl-a	–	$3 - bandindex = (Rrs(681.25))^{-1} - (Rrs(708.75))^{-1}) \times (Rrs(753.75))^{-1}$	$R^2: 0.74$	–	Bresciani et al. (2017)
MERIS	DL	Chl-a	April and September 2002-2012	Free University Berlin (FUB)	r: 0.9	–	Philipson et al. (2016)
		TSM			r: 0.87		
		TUR			r: 0.89		
MERIS	EM	Chl-a	April 2008	$Chla = a \times \frac{Rrs(708)}{Rrs(664)}^b$	$R^2: 0.964$	–	Matthews et al. (2010)
		TSS		$TSS = -a + b \times (\frac{Rrs(708)}{Rrs(559)}) + Rrs(664)$	$R^2: 0.76$		
		SDD		$SDD = a - b \times \frac{Rrs(708)}{Rrs(664)}$	$R^2: 0.801$		
		CDOM		$CDOM = -a - b \times \frac{Rrs(708)}{Rrs(664)}$	$R^2: 0.751$		
MODIS	EM	Chl-a	May to November 2006	$Chl - a = a - b \times \frac{Rrs(443)}{Rrs(551)}$	$R^2: 0.582$	–	Chavula et al. (2009)
MODIS	EM	SDD	May to October 2006	$ln(SDD) = a - b \times Rrs(645) + c \times Rrs(469)$	$R^2: 0.32 - 0.71$	$R^2: 0.63 - 0.73$	Knight and Voth (2012)

Table 4 continued

Sensor	Method	Parameter(s)	Temporal observation	Band/equation	Training Acc	Validation Acc	Ref
MODIS	EM	SDD	1970–2009	$ln(SDD) = a \times Rrs(645) + b \times Rrs(469) + c \times avgdepth + d \times wetland + e$	$R^2 : 0.71 - 0.94$	–	McCullough et al. (2012)
MODIS	EM	TSM	March to Jun 2007, 2008, 2009	$Singleband: Rrs(645)$	$R^2 : 0.461$	–	Tarrant et al. (2010)
				$Singleband: Rrs(856)$	$R^2 : 0.521$		
MODIS	EM	TSS	27 November 2010, 13 May 2011, and 7 November 2011	$TSS = a \times Rrs(858) - b$	$R^2 : 0.95$	RMSE: 16.5	Kaba et al. (2014)
		TUR		$TUR = a \times Rrs(858) - b$	$R^2 : 0.89$	RMSE: 16.5	
		SDD		$SDD = a \times e^{(-b \times Rrs(858))}$	$R^2 : 0.74$	RMSE: 0.11	
CZCS, SeaWiFS, and MODIS	EM	SDD	1979–1985, 1998–2004, and 2005–2014	$SDD^{-1} = a \times eRrs(550)^3 - b \times Rrs(550)^2 + c \times Rrs(550) + d$	$R^2 : 0.74$	–	Binding et al. (2015)
Sentinel-3 OLCI	ML	SDD	2016–2018	Random forest	$R^2 :> 0.92$	$R^2 :> 0.60$	Shen et al. (2020)
Sentinel-3 OLCI	EM	POC	–	$POC = a \times \frac{Rrs(510)}{Rrs(681.25)}$	RMSE: 3.33	RMSE: 2.13	Lin et al. (2018)
				$POC = a \times ((Rrs(665)^{-1} - Rrs(708.75)^{-1}) \times Rrs(753.75))$	RMSE: 3.2	RMSE: 2.13	

*Where a, b, and c are coefficients obtained from regression analysis. The coefficients may vary from image to image. Additionally, the abbreviations EM, SA, DL, and ML denote the empirical model, semi-analytical model, deep learning approach, and machine learning approach, respectively

Table 5 Retrieval models using medium to high spatial resolution satellite multispectral data

Sensor	Method	Parameter(s)	Temporal observation	Band/equation	Training Acc	Validation Acc	Ref
RapidEye	EM	EC, TDS, SDD, SDD, TUR	12-Aug-14	$Bandratio: \frac{Rrs(440-510)}{Rrs(760-850)}$	$r :> 0.56$ & < -0.55	–	Avdan et al. (2019)
		SPM, and Chl-a					
World View-2	EM	pH, DO, TDS, TSS, TA, OP	2010 and 2011	Single bands	$R^2 : 0.19 - 0.82$	–	El Saadi et al. (2014)
		COD, BOD, and					
		Chl-a					
ASTER	EM	Chl-a	9-Jun-05	$Chl - a = a + b \times Rrs(520-600) - c \times Rrs(630-069) - d \times Rrs(780-860) + e \times Rrs(1600 - 1700)$	$R^2 : 0.863$	–	Nas et al. (2009)
IKONOS	EM	SDD	4-Sep-01	$ln(SDD) = a \times \frac{Rrs(445-516)}{Rrs(632-698)} - b \times Rrs(445 - 516) - c$	$R^2 : 0.89$	–	Sawaya et al. (2003)
Landsat5 TM	EM	Algae, TUR, N, NH3-N, NO3-N, TP, DP, COD	2005	Stepwise multiple linear regression	–	r: 0.613–0.955	He et al. (2008)
Landsat5 TM	EM	Chl-a, TUR, SDD, and TSS	22-Aug-06	Single band, band ratio, combination	$R^2 : 0.60 - 0.71$	–	Nas et al. (2010)
Landsat5 TM	SA	TSM	19-Feb-06	Spectral decomposition algorithm	$R^2 : 0.63 - 0.74$	RMSE: 0.11	Zhou et al. (2008)
Landsat5 TM	EM	Chl-a	28-Oct-03, 4-Mar-04	Single band and band ratio	$R^2 : 0.87$	–	Oyama et al. (2009)
Landsat5 TM	EM	Chl-a	2000	Band ratios	$R^2 : 0.85 - 0.89$	–	Brezonik et al. (2005)
		CDOM		Single band and band ratios	$R^2 : 0.60 - 0.71$		

Table 5 continued

Sensor	Method	Parameter(s)	Temporal observation	Band/equation	Training Acc	Validation Acc	Ref
Landsat TM	DL	Chl-a	Dec and July in 98, 99, 10	Neural network (NN)	RMSE: 0.03–0.54	RMSE: 0.03–0.14	Chebud et al. (2012)
Landsat TM	EM	Chl-a	14-Oct-04	$Bandratio: \frac{Rrs(760)}{Rrs(630)}$	$R^2: 0.67$	–	Duan et al. (2007)
Landsat TM and 7 ETM+	SEM	Chl-a	2003–2010	$ln(Chl-a) = a + b \times Rrs(520) + c \times Rrs(630) + d \times WST$	$R^2: 0.72$	$R^2: 0.88$	Bonansea et al. (2015)
Landsat7 and 8 OLI	EM	Chl-a	2013–2018	$log(chl-a) = a - b \times \frac{lnRrs(630)}{lnRrs(1550)} + c \times \frac{Rrs(630)}{Rrs(520)} - d \times \frac{ln(Rrs(630)}{ln(Rrs(450)}$	$R^2: 0.75$	RMSE: 0.02	(Markogianni et al., 2020)
Landsat8 OLI	EM	SDD	2016–2017	Single band and band ratio	$R^2: 0.89$	$R^2: 0.84$	Bonansea et al. (2018)
Landsat7 ETM+	EM	Chl-a	27-Mar-03	$ln(Chl-a) = a - b \times lnRrs(450) + c \times lnRrs(520)$	$R^2: 0.723$	–	Kabbara et al. (2008)
		TUR		$ln(Tur) = a - b \times lnRrs(450) + c \times lnRrs(520)$	$R^2: 0.57$		
		SDD		$ln(SDD) = -a + b \times lnRrs(450) + c \times lnRrs(520)$	$R^2: 0.54$		
Landsat7 ETM+	SA	TUR	1999 to 2022	Bio-optical model calibration	$R^2: 0.67$	$R^2: 0.72$	Di Vittorio et al. (2023)
		TSS			$R^2: 0.71$	$R^2: 0.74$	
Landsat5 TM and SPOT	SA	TSM	24 May, 11 July, 2 and 12 Aug 1995	Bio-optical model	$R^2: 0.99$	–	Dekker et al. (2001)
Sentinel-2A	EM	SDD	2017	$Bandratio: Rrs(490), \frac{Rrs(560)}{Rrs(842)}$	$R^2: 0.88$	$R^2: 0.85$	Bonansea et al. (2018)
Sentinel-2A	SA	Chl-a	Aug 2015	$Chl-a: Rrs(705) - (Rrs(665) + \frac{Rrs(705)}{2}$	$R^2: 0.83$	–	Toming et al. (2016)
Sentinel-2A	ML	SDD	2003–2021	Random forest	RMSE: 0.27	RMSE: 0.10	Maciel et al. (2021)
Sentinel-2A	ML	TSS	2017–2018	Cubist	$R^2: 0.96$	$R^2: 0.80$	Saberioon et al. (2020)

*Where a, b, and c are coefficients obtained from regression analysis. The coefficients may vary from image to image. Additionally, the abbreviations EM, SEM, SA, DL, and ML denote the empirical model, semi-empirical model, semi-analytical model, deep learning approach, and machine learning approach, respectively

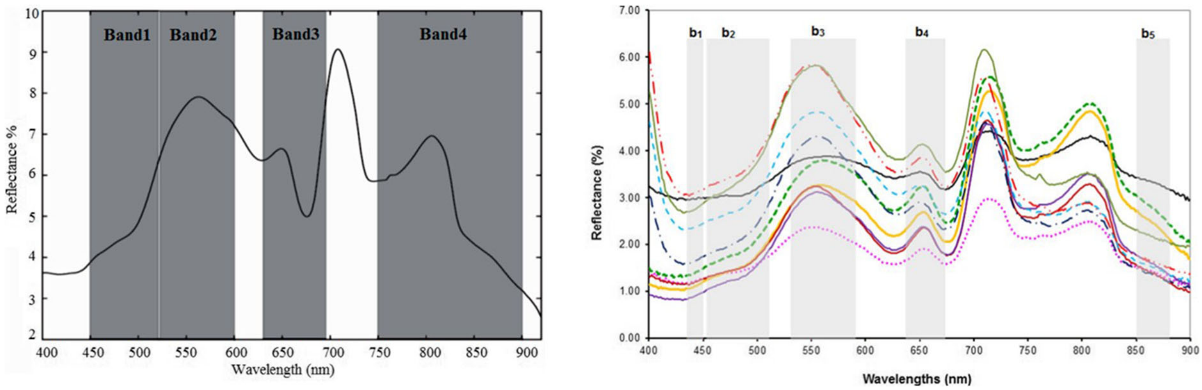

Fig. 6 Example of chlorophyll-a reflection in relation to band positions of Landsat-7 ETM+ (left) (Gholizadeh et al., 2016) and Landsat 8 OLI (right) (Ha et al., 2017). The different colors in the right image represent chlorophyll-a reflectance in nine lakes

temperature, pH, turbidity, oxidation-reduction potential (ORP), specific conductivity, high dissolved oxygen (HDO), crude oil contamination (Rostom et al., 2017), chlorophyll-a concentration (Murugan et al., 2016), total suspended solids (Tan et al., 2011; Wu et al., 2014), and colored dissolved organic matter (CDOM) (Moses et al., 2015). Hyperspectral satellite sensors that have been used in water quality studies include Hyperion on NASA EO-1 and PRecursore IperSpettrale della Missione Applicativa (PRISMA), and some retrieval models using hyperspectral satellite data are presented in Table 6.

Although hyperspectral imaging offers high spectral resolution, allowing for precise identification and measurement of water quality parameters, data processing can be complex. Zhong et al. (2021) noted that one challenge is the spectral combination problem, where multiple parameters can contribute to a single spectral signature. This makes it difficult to isolate and quantify individual parameters accurately. Another limitation of hyperspectral satellite data is its limited availability, especially for specific regions or sensors (Yang et al., 2022). This can restrict the temporal resolution of water quality monitoring in small water bodies. Similar to multispectral satellite sensors, noise and atmospheric influences and coarse spatial resolution can further complicate the analysis of hyperspectral data. These challenges can be addressed through the use of advanced data processing techniques and algorithms, as well as through the development of new and improved remote sensing technologies.

Limitations of satellite remote sensing

The use of satellite remote sensing in monitoring water quality parameters in inland water bodies has been tested and applied in several individual studies. However, developing operational and widely applicable monitoring tools is difficult due to several drawbacks.

The correction of atmospheric effects in satellite images is vital as most reflectance comes from the atmosphere (Hussein & Assaf, 2020; Moses et al., 2017). Failure to do so may lead to inaccuracies in water quality measurements. Atmospheric corrections, on the other hand, may significantly impact the satellite product (Harvey et al., 2015) and lead to uncertainty (Bresciani et al., 2017; Castro et al., 2020; El Saadi et al., 2014; Toming et al., 2016). This uncertainty is attributed to different factors, such as variations in atmospheric conditions (Werdell et al., 2010), the complexity of inland water bodies (IOCCG, 2018; Shen et al., 2020), and errors in atmospheric correction algorithms (Kutser, 2012). It has been observed that using top-of-atmosphere (TOA) measurements instead of atmospherically corrected data or bottom-of-atmosphere (BOA) data can yield better results (Grendaitė et al., 2018; Kutser, 2012; Tebbs et al., 2013; Toming et al., 2016).

In addition, the use of land-based atmospheric correction algorithms on water surfaces may lead to significant errors (Grendaitė et al., 2018; Maciel et al., 2021; Toming et al., 2016) due to the distinct optical properties and atmospheric effects specific to water (Bonansea

Table 6 Retrieval models using hyperspectral satellite data

Sensor	Method	Parameter(s)	Temporal observation	Band/equation	Training Acc	Validation Acc	Ref
Hyperion	SA	Chl-a	22-Jun-03	Matrix inversion method (MIM)	$R^2 : 0.59$	–	Giardino et al. (2007)
		TUR			$R^2 : 0.57$		
Hyperion	EM	Chl-a	January and April 2013	$Bandratio: \frac{Rrs(467)}{Rrs(548)}$	$R^2 : 0.707$	RMSE: 2.47	Flores-Anderson et al. (2020)
HICO	DL	Chl-a	2011 and 2014	Mixture density networks (MDN)	Bias: −3	Bias: −0.3	Pahlevan et al. (2021)
HICO	SA	PC	2009–2014	$PC = a \times (\frac{Rrs(668)}{Rrs(708)})^b$	$R^2 : 0.63$	–	Dev et al. (2022)
		Chl-a		$Chl - a = a \times (\frac{Rrs(708)}{Rrs(668)})^b$	$R^2 : 0.88$		
HICO	DL	Chl-a, TSS	2009–2019	Deep neural network (DNN)	$R^2 :> 0.93$	$R^2 :> 0.91$	Banerjee and Shanmugam (2021)
ZY1-02D	ML	DO, CDOM, P	September 2018 to November 2021	XGBoost	$R^2 : 0.48$	RMSE: 0.10–4.77	Yang et al. (2022)

*Where a, b, and c are coefficients obtained from regression analysis. The coefficients may vary from image to image. Additionally, the abbreviations EM, SA, DL, and ML denote the empirical model, semi-analytical model, deep learning approach, and machine learning approach, respectively

et al., 2015; Liu et al., 2016). Several studies have compared the performance of land-based atmospheric correction algorithms with specialized algorithms developed for water quality studies (Ansper & Alikas, 2018; Rodrigues et al., 2017). For example, Wang et al. (2019) recommend the use of water-specific atmospheric correction algorithms, such as the EXP atmospheric algorithm (based on exponential extrapolation) that is integrated into the ACOLITE algorithm, to improve the accuracy of satellite-based water quality monitoring. In parallel, a study by Pahlevan et al. (2021) that evaluated the performance of different water-based atmospheric correction methods for Landsat-8 and Sentinel-2 over various water bodies, including lakes, rivers, and coastal waters, showed a performance difference of water-specific algorithms in different optical characteristics of inland waters. Therefore, specialized water-specific atmospheric correction algorithms should be used to ensure accurate monitoring of water parameters. The choice of the atmospheric correction method should consider the specific characteristics of the water body and the goals of the analysis (Pahlevan et al., 2021; Tyler et al., 2006). Similarly, validation of the atmospheric correction outputs against ground-based measurements is necessary to assess accuracy and quality.

The impact of cloud coverage on satellite images results in data gaps (Bonansea et al., 2015) and limits the availability of suitable images for analysis (Cheng et al., 2020; Olivetti et al., 2020), particularly during winter and rainy seasons. Small water bodies are especially susceptible to cloud coverage, making it challenging to obtain consistent and representative satellite imagery. The frequent occurrence of clouds and haze can further complicate the study of small areas and hinder the monitoring of water quality parameters (Olivetti et al., 2020).

Satellite remote sensing data with both high spatial and spectral resolution, suitable for water quality studies, is currently limited (Palmer et al., 2015). Many multispectral sensors mounted on satellites show potential for evaluating water quality parameters, such as Sentinel-2 and Landsat series data, which have comparable high spatial and low spectral resolution (Brezonik et al., 2009). However, their spatial resolution is generally not high enough to study small inland water bodies (McCullough et al., 2012). Moreover, sensors built solely for aquatic remote sensing, like MODIS and MERIS, have valuable narrow wavelength bands for global-scale water quality assessments (Hellweger et al., 2004; Sayers et al., 2015), but they also have limitations in studying small inland water bodies (Keith et al., 2014; Tyler et al., 2006). The lack of high spatial and spectral resolution data poses a challenge in accurately monitoring water quality parameters.

The temporal resolution of satellite remote sensing data is another significant challenge in water quality monitoring. Obtaining high temporal resolution satellite imagery for water quality studies is often not readily available. There is usually a temporal gap between satellite imagery and in situ measurements, which could be a few days to weeks, making it difficult to develop accurate regression models between water quality parameters and satellite data. For instance, Harvey et al. (2015) used MERIS images with a 0–3-day gap, while Kutser et al. (2016) obtained Sentinel-2 and Landsat-8 images with a 3-day gap. He et al. (2008) used the closest Landsat-5 images with a 9-day gap, and in some cases, it was challenging to find imagery that approximated the date of field measurement (Toming et al., 2016). Bonansea et al. (2015) noted that the maximum time lag between in situ measurements and satellite overpass should be no more than 1 day to ensure effective matching. Larger time lags may lead to discrepancies between the field measurements and satellite data, resulting in less accurate estimation of water quality parameters (Kabiri, 2023). Furthermore, it is difficult to observe rapid changes in the trophic state of water bodies, such as algal blooms, with satellite imagery due to its lower temporal resolution (Gholizadeh et al., 2016; Kloiber et al., n.d.; McCullough et al., 2012; Sayers et al., 2015; Su et al., 2015).

The limited availability of satellite imagery with high spectral, spatial, and temporal resolution has been a significant challenge in studying water quality parameters in small water bodies. To address this issue, some researchers have proposed data fusion of multiple satellite images to combine the advantages of the high spatial, spectral, and temporal resolution (Castro et al., 2020; Fu et al., 2018; Lai et al., 2021). However, this approach can be computationally demanding (Yulong et al., 2022). In studies conducted by Hellweger et al. (2004) and Niroumand-Jadidi et al. (2020), it was concluded that achieving satellite images with all three resolutions is nearly impossible due to signal-to-noise conditions. As a result, unmanned aerial vehicles (UAVs) have emerged as a promising alternative for conducting measurements instead of relying solely on satellite-based observation (Brezonik et al., 2009). UAVs have the potential to provide high-resolution images with improved spatial and temporal resolution based on the quality of their onboard sensors and camera capabilities. This allows researchers to overcome some of the limitations posed by satellite imagery. UAVs also have the ability to capture data with greater detail, enabling the detection of water quality parameters such as harmful algal blooms and pollutants at small scales.

Unmanned aerial vehicle (UAV) remote sensing

Unmanned aerial vehicles (UAVs) have emerged as a promising tool for water quality monitoring, providing high-resolution images with a spatial resolution of up to a few centimeters (Olivetti et al., 2020). This enhanced resolution enables the detailed and accurate mapping of water quality parameters, allowing for the detection of subtle changes in water quality that might be missed. Furthermore, the versatility of UAVs in capturing images at different times of the day facilitates the monitoring of diurnal cycles and can provide information on daily fluctuations in temperature, dissolved oxygen, and pH (Castro et al., 2020). One of the key advantages of UAVs is their ability to bridge the gap between in situ sampling and satellite sensors; UAVs offer a unique way to obtain water quality data at the local scale while also integrating with regional and global data sets obtained from satellites (Isgró et al., 2022). These reasons make UAVs an attractive alternative for water quality monitoring, particularly for small waterbodies that are not well served by satellite data. In recent years, several studies have explored the use of UAV remote sensing data for water quality monitoring (Castro et al., 2020; Cui et al., 2022; Guimarães et al., 2019; Olivetti et al., 2020; Zhang et al., 2023).

Multispectral remote sensing

Various multispectral remote sensing sensors such as Canon Powershot S110 and RedEdge Micasense have been used for water quality studies. In Table 7, the use of multi-temporal imagery from UAV remote sensing data shows good performance with R^2 ranging from 0.84 to 0.94, and higher R^2 values are observed for single images, ranging from 0.86 to 1.

Hyperspectral remote sensing

Similarly, hyperspectral UAV remote sensing has been used to monitor water quality parameters, as shown in Table 8. The results of these studies have demonstrated satisfactory performance with R^2 ranging from 0.94 to 0.96 using multi-temporal imagery and 0.72 to 0.955 using single-date images. These findings suggest that UAV-based models can be used to expand water quality databases in both space and time.

Discussion

The studies reviewed in this paper demonstrate a strong agreement between remote sensing-driven values and field measurements, indicating the potential of remote sensing-based water quality algorithms in Case II water bodies. However, it is important to consider several factors that contribute to the consistency and robustness of these algorithms.

One significant challenge in developing robust water retrieval algorithms is the sample size. Inland water bodies exhibit spatial and temporal variability influenced by factors such as land use and point source pollution. Obtaining a small sample size can introduce potential biases in assessing water quality conditions. Several studies (mentioning some (Avdan et al., 2019; Bonansea et al., 2018; Bresciani et al., 2017; Harvey et al., 2015; Lai et al., 2021; Ma & Dai, 2007)) have relied on small sample sizes to build their remote sensing-based water quality algorithms, with only a few surface waters considered in each study. Limited observations make it difficult to capture the complex nature of inland water, resulting in reduced statistical power, which hampers drawing robust conclusions and making accurate predictions. Moreover, small sample sizes pose challenges in obtaining a sufficient number of ground truth measurements for validation purposes (Fu et al., 2018; Moses et al., 2009), which ultimately hinders effective management and mitigation strategies.

Validation plays a crucial role in establishing the accuracy and reliability of remote sensing water retrieval algorithms. It provides insights into how well algorithms capture specific optical properties and helps identify their strengths, weaknesses, and potential areas for improvement (Yen et al., 2015). However, several studies have neglected the validation step (El Saadi et al., 2014; Gons et al., 2008; Kloiber et al., n.d.; Nas et al., 2010), possibly due to limited sample sizes, as calibration and validation require a large dataset. This limitation can make it challenging to perform cross-

Table 7 Retrieval models using UAV multispectral data

Sensor	Method	Parameter(s)	Temporal observation	Band/equation	Training Acc	Validation Acc	Ref
Canon Powershot S110	EM	Chl-a	24-Nov-14	$ln(Chl-a) = a \times \frac{Rrs(850)}{Rrs(660)}) + b$	$R^2 : 1$	–	Su et al. (2015)
		P		$ln(P) = a \times \frac{Rrs(850)}{Rrs(660)})$	$R^2 : 0.997$		
		SDD		$ln(P) = a \times \frac{Rrs(850)}{Rrs(450)})$	$R^2 : 0.998$		
Canon ELPH 110HS	EM	Chl-a	1-Mar-16	$Chl-a = a + b \times \frac{Rrs(560)}{Rrs(680)} + c \times \frac{Rrs(708)}{Rrs(680)}$	$R^2 : 0.86$	–	Guimarães et al. (2017)
Canon ELPH 110HS	DL	TSS	March 2016 and 2017	Artificial neural network (ANN)	$R^2 : 0.84$	$R^2 : 0.57$	Guimarães et al. (2019)
Parrot Sequoia	EM	TSS	March–Dec/2018	Single band (Rrs (790))	$R^2 : 0.94$	–	Olivetti et al. (2020)
RedEdge Micasense	EM	Chl-a	19 Sept 2017 and 2 Oct 2018	$Threeband: Rrs(560) - \frac{Rrs(475)}{Rrs(560)} + Rrs(475)$	$R^2 : 0.85$	$R^2 : 0.98$	Castro et al. (2020)

*Where a, b, and c are coefficients obtained from regression analysis. The coefficients may vary from image to image. Additionally, the abbreviations EM, SA, DL, and ML denote the empirical model, semi-analytical model, deep learning approach, and machine learning approach, respectively

Table 8 Retrieval models using UAV hyperspectral data

Sensor	Method	Parameter(s)	Temporal observation	Band/equation	Training Acc	Validation Acc	Ref
Gaia Sky-mini	DL	P, N, COD, BOD, TUR, and Chl-a	–	Self-adapting selection of multiple neural networks (SSNN)	$R^2 : 0.929 - 0.978$	$R^2 : 0.9255 - 0.990$	Zhang et al. (2020)
Headwall NANO-Hyperspec	ML	Chl-a	9 to 10 September 2018	Catboost regression (CBR)	$R^2 : 1$	$R^2 : 0.96$	Lu et al. (2021)
		TSS			$R^2 : 0.95$	$R^2 : 0.94$	
Gaiasky-mini2-VN	EM	TUR	–	Partial least squares regression model	$R^2 : 0.98$	$R^2 : 0.72$	Cui et al. (2022)
Gaia Sky-M	DL	P, N, COD, BOD, Chl-a, TSS, and TUR	11-Oct-21	Graph convolution network (GCN)	–	$R^2 : 0.8 - 0.955$	Zhang et al. (2023)
Gaia Sky-M	DL	P, N, COD, BOD, and Chl-a	3-Sep-19	Hybrid feedback deep factorization machine (HF-DFM)	–	$R^2 : 0.72 - 0.93$	Zhang et al. (2021)

*Where a, b, and c are coefficients obtained from regression analysis. The coefficients may vary from image to image. Additionally, the abbreviations EM, SA, DL, and ML denote the empirical model, semi-analytical model, deep learning approach, and machine learning approach, respectively

comparisons between different sensors, platforms, and algorithms. Further, the absence of validation deprives researchers of the opportunity to identify and address deficiencies in sensors, platforms, or algorithms.

A commonly used approach in water quality assessment is the utilization of a single-date or single-image model, where a single snapshot of the water body is used. This approach can be practical when continuous monitoring or extensive temporal coverage is not required. The literature review indicates the good performance of these approaches under optimal conditions. However, water quality parameters often exhibit significant temporal variations influenced by seasonal cycles, diurnal patterns, and occasional events. By relying solely on a single-date approach, these variations are not captured, potentially leading to an incomplete understanding of the dynamics and trends of water quality over time. Furthermore, due to the fact that these models are sensitive to water-specific characteristics and the atmospheric conditions of the day, they can not necessarily be applied to other places or time frames (Rubin et al., 2021).

Conclusion

The use of remote sensing data offers advantages over conventional water quality assessment techniques, which often necessitate extensive fieldwork and costly laboratory analysis. Based on the comprehensive review conducted, it can be concluded that the advancements in remote sensing technology can support the monitoring, assessment, and estimation of various water quality parameters, including CDOM, Chl-a, TSS, TS, SD, and turbidity, among others. Several retrieval algorithms are frequently employed, such as empirical, semi-analytical, and artificial intelligence approaches.

The development of multispectral and hyperspectral satellite sensors has played a significant role in this regard, enabling high-resolution spatial and temporal observations of water bodies and offering valuable insights into variations in water quality. The integration of UAVs in remote sensing has significantly addressed limitations of low spatial and temporal resolution, atmospheric effects, and cloud conditions. UAV imagery provides high spatial resolution by operating at flexible and low-flight altitudes. This capability allows for the detection of short-term changes in small water bodies and facilitates the measurement and monitoring of water quality with the appropriate spatial and temporal resolution, even under challenging climatic conditions like clouds or haze.

Overall, this review provides a comprehensive overview of the current knowledge and applications of remote sensing in inland water quality assessment. Additionally, it offers invaluable insights into data preprocessing and analysis techniques and the limitations of remote sensing approaches in inland water quality assessment. These insights can guide researchers in selecting from alternative remote sensing approaches for water quality assessments in inland water bodies.

Appendix

The complete review on inland water quality monitoring using remote sensing can be found here: https://docs.google.com/spreadsheets/d/1EjM1Vl48Hi8oavK2QOxnVm7TMyFpgdBn/edit?usp=sharing&ouid=111951620892723892246&rtpof=true&sd=true.

Acknowledgements The authors would like to thank the anonymous reviewers for their insightful comments and constructive feedback, which greatly contributed to the refinement and improvement of this paper.

Author contributions ETW: writing—original draft. LHB: supervision, writing—review and editing. CADV: writing—review and editing.

Funding This work was supported in part by the National Oceanic and Atmospheric Administration (NOAA) Award, (Grant numbers NA21OAR4590358) and National Science Foundation (NSF) grant 1800768.

Data availability Not applicable

Declarations

Ethical approval All authors have read, understood, and have complied as applicable with the statement on “Ethical responsibilities of Authors” as found in the Instructions for Authors and are aware that with minor exceptions, no changes can be made to authorship once the paper is submitted.

Conflict of interest The authors declare no competing interests.

References

Abdelmalik, K. W. (2018). Role of statistical remote sensing for inland water quality parameters prediction. *The Egyptian Journal of Remote Sensing and Space Science, 21*(2), 193–200. https://doi.org/10.1016/J.EJRS.2016.12.002

Ansper, A., & Alikas, K. (2018). Retrieval of chlorophyll a from Sentinel-2 MSI data for the European union water framework directive reporting purposes. *Remote Sensing, 11*(1), 64. https://doi.org/10.3390/RS11010064

Arias-Rodriguez, L. F., Duan, Z., Díaz-Torres, J.d.J., Basilio Hazas, M., Huang, J., Kumar, B.U., . . . Disse, M. (2021). Integration of remote sensing and Mexican water quality monitoring system using an extreme learning machine. *Sensors, 21*(12), 4118. https://doi.org/10.3390/s21124118

Avdan, Z. Y., Kaplan, G., Goncu, S., & Avdan, g. (2019). Monitoring the water quality of small water bodies using high-resolution remote sensing data. *ISPRS International Journal of Geo-Information, 8*(12), 553. https://doi.org/10.3390/IJGI8120553

Banerjee, S., & Shanmugam, P. (2021). Novel method for reconstruction of hyperspectral resolution images from multispectral data for complex coastal and inland waters. *Advances in Space Research, 67*(1), 266–289. https://doi.org/10.1016/J.ASR.2020.09.045

Binding, C. E., Greenberg, T. A., Watson, S. B., Rastin, S., & Gould, J. (2015). Long term water clarity changes in north America's great lakes from multi-sensor satellite observations. *Limnology and Oceanography, 60*(6), 1976–1995. https://doi.org/10.1002/LNO.10146

Bonansea, M., Ledesma, C., Rodríguez, C., Pinotti, L., & Antunes, M. H. (2015). Effects of atmospheric correction of Landsat imagery on lake water clarity assessment. *Advances in Space Research, 56*(11), 2345–2355. https://doi.org/10.1016/J.ASR.2015.09.018

Bonansea, M., Ledesma, M., Rodriguez, C., & Pinotti, L. (2018). Using new remote sensing satellites for assessing water quality in a reservoir. *Hydrological Sciences, 64*(1), 34–44. https://doi.org/10.1080/02626667.2018.1552001

Bonansea, M., Rodriguez, M. C., Pinotti, L., & Ferrero, S. (2015). Using multi-temporal Landsat imagery and linear mixed models for assessing water quality parameters in Río Tercero reservoir (Argentina). *Remote Sensing of Environment, 158*, 28–41. https://doi.org/10.1016/J.RSE.2014.10.032

Bresciani, M., Giardino, C., Stroppiana, D., Dessena, M. A., Buscarinu, P., Cabras, L., . . . Tzimas, A. (2019). Monitoring water quality in two dammed reservoirs from multispectral satellite data. *European Journal of Remote Sensing, 52*(sup4), 113–122. https://doi.org/10.1080/22797254.2019.1686956

Bresciani, M., Vascellari, M., Giardino, C., & Matta, E. (2017). Remote sensing supports the definition of the water quality status of lake Omodeo (Italy). *European Journal of Remote Sensing, 45*(1), 349–360. https://doi.org/10.5721/EuJRS20124530

Brezonik, P., Menken, K. D., & Bauer, M. (2005). Landsat-based remote sensing of lake water quality characteristics, including chlorophyll and colored dissolved organic matter (CDOM). *Lake and Reservoir Management, 21*(4), 373–382. https://doi.org/10.1080/07438140509354442

Brezonik, P., Menken, K. D., & Bauer, M. (2009). Landsat-based remote sensing of lake water quality characteristics, including chlorophyll and colored dissolved organic matter (CDOM). *Lake and Reservoir Management, 21*(4), 373–382. https://doi.org/10.1080/07438140509354442

Bukata, R. P. (2005). *Satellite monitoring of inland and coastal water quality: Retrospection, introspection, future directions*. CRC Press.

Cao, Z., Ma, R., Duan, H., Pahlevan, N., Melack, J., Shen, M., & Xue, K. (2020). A machine learning approach to estimate chlorophyll-a from Landsat-8 measurements in inland lakes. *Remote Sensing of Environment, 248*, 111974, https://doi.org/10.1016/J.RSE.2020.111974

Carvalho, B. C., De Fortunato, H. F., & Figueira, R. M. (2022). Water quality analysis on the Três Irmãos HPP reservoir (SP, Brazil) using Landsat-8 satellite imagery. *Inter national Geoscience and Remote Sensing Symposium (IGARSS), 3331–3334*,. https://doi.org/10.1109/IGARSS46834.2022.9884641

Castro, C. C., Gómez, J. A. D., Martín, J. D., Sánchez, B. A. H., Arango, J. L. C., Tuya, F. A. C., & Díaz-Varela, R. (2020). An UAV and satellite multispectral data approach to monitor water quality in small reservoirs. *Remote Sensing, 12*(9), 1514. https://doi.org/10.3390/RS12091514

Chang, N.-B., & Vannah, B. (2013). Comparative data fusion between genetic programing and neural network models for remote sensing images of water quality monitoring. *Proceedings - 2013 IEEE International Conference on Systems, Man, and Cybernetics,* 1046–1051, https://doi.org/10.1109/SMC.2013.182

Chavula, G., Brezonik, P., Thenkabail, P., Johnson, T., & Bauer, M. (2009). Estimating chlorophyll concentration in lake Malawi from MODIS satellite imagery. *Physics and Chemistry of the Earth, Parts A/B/C, 34*(13–16), 755–760. https://doi.org/10.1016/J.PCE.2009.07.015

Chebud, Y., Naja, G. M., Rivero, R. G., & Melesse, A. M. (2012). Water quality monitoring using remote sensing and an artificial neural network. *Water, Air, & Soil Pollution, 223*, 4875–4887. https://doi.org/10.1007/s11270-012-1243-0

Cheng, K. H., Chan, S. N., & Lee, J. H. W. (2020). Remote sensing of coastal algal blooms using unmanned aerial vehicles (UAVs). *Marine Pollution Bulletin, 152*,. https://doi.org/10.1016/j.marpolbul.2020.110889

Cui, M., Sun, Y., Huang, C., & Li, M. (2022). Water turbidity retrieval based on UAV hyperspectral remote sensing. *Water 2022,* 14 (1), 128, https://doi.org/10.3390/W14010128

Dekker, A. G., Vos, R. J., & Peters, S. W. M. (2001). Comparison of remote sensing data, model results and in situ data for total suspended matter (TSM) in the Southern Frisian lakes. *Science of The Total Environment, 268*(1–3), 197–214. https://doi.org/10.1016/S0048-9697(00)00679-3

Del Pozo, S., Rodríguez-Gonzálvez, P., Hernández-López, D., & Felipe-García, B. (2014). Vicarious radiometric calibration of a multispectral camera on board an unmanned aerial system. *Remote Sensing, 6*(3), 1918–1937. https://doi.org/10.3390/RS6031918

Dev, P. J., Sukenik, A., Mishra, D. R., & Ostrovsky, I. (2022). Cyanobacterial pigment concentrations in inland waters: Novel semi-analytical algorithms for multi- and hyperspectral remote sensing data. *Science of The Total Environment, 805*, 150423. https://doi.org/10.1016/J.SCITOTENV.2021.150423

Di Vittorio, C. A., Moerk, M., & Kreutzberger, W. (2023). Enhancing perspectives on lake impairments using satellite observations: A case study on high rock lake, North Carolina. *JAWRA Journal of the American Water Resources*

Association, 59(5), 1067–1083. https://doi.org/10.1111/1752-1688.13127

Doerffer, R., Sorensen, K., & Aiken, J. (1999). MERIS potential for coastal zone applications. *International Journal of Remote Sensing, 20*(9), 1809–1818. https://doi.org/10.1080/014311699212498

Dosskey, M.G. (2001). Toward quantifying water pollution abatement in response to installing buffers on crop land. *Environmental Management* 2001 28:5, 28 (5), 577–598, https://doi.org/10.1007/S002670010245

Dörnhöfer, K., & Oppelt, N. (2016). Remote sensing for lake research and monitoring - Recent advances. *Ecological Indicators, 64*, 105–122. https://doi.org/10.1016/J.ECOLIND.2015.12.009

Duan, H., Zhang, Y., Zhang, B., Song, K., & Wang, Z. (2007). Assessment of chlorophyll-a concentration and trophic state for lake Chagan using Landsat TM and field spectral data. *Environmental Monitoring and Assessment, 129*, 295–308. https://doi.org/10.1007/S10661-006-9362-Y

Elbeih, S. F. (2015). An overview of integrated remote sensing and GIS for groundwater mapping in Egypt. *Ain Shams Engineering Journal, 6*(1), 1–15. https://doi.org/10.1016/J.ASEJ.2014.08.008

El Saadi, A. M., Yousry, M. M., & Jahin, H. S. (2014). Statistical estimation of Rosetta branch water quality using multi-spectral data. *Water Science, 28*(1), 18–30. https://doi.org/10.1016/J.WSJ.2014.10.001

Flores-Anderson, A. I., Griffin, R., Dix, M., Romero-Oliva, C. S., Ochaeta, G., Skinner-Alvarado, J., . . . Barreno, F. (2020). Hyperspectral satellite remote sensing of water quality in lake Atitlán, Guatemala. *Frontiers in Environmental Science, 8*, 1–13. https://doi.org/10.3389/fenvs.2020.00007

Frappart, F., Seyler, F., Martinez, J. M., León, J. G., & Cazenave, A. (2005). Floodplain water storage in the Negro River basin estimated from microwave remote sensing of inundation area and water levels. *Remote Sensing of Environment, 99*(4), 387–399. https://doi.org/10.1016/J.RSE.2005.08.016

Fu, Y., Xu, S., Zhang, C., & Sun, Y. (2018). Spatial downscaling of MODIS chlorophyll-a using Landsat 8 images for complex coastal water monitoring. *Estuarine, Coastal and Shelf Science, 209*, 149–159. https://doi.org/10.1016/J.ECSS.2018.05.031

Fukushima, T., Matsushita, B., Oyama, Y., Yoshimura, K., Yang, W., Terrel, M., . . . Takegahara, A. (2016). Semi-analytical prediction of Secchi depth using remote-sensing reflectance for lakes with a wide range of turbidity. *Hydrobiologia, 780*(1), 5–20. https://doi.org/10.1007/S10750-015-2584-7

Gebrehiwot, A. A., & Hashemi-Beni, L. (2021). Three-dimensional inundation mapping using UAV image segmentation and digital surface model. *ISPRS International Journal of Geo-Information, 10*(3), 144. https://doi.org/10.3390/ijgi10030144

Gholizadeh, M. H., Melesse, A. M., & Reddi, L. (2016). A comprehensive review on water quality parameters estimation using remote sensing techniques. *Sensors, 16*(8), 1298. https://doi.org/10.3390/S16081298

Giardino, C., Brando, V.E., Dekker, A.G., Strömbeck, N., & Candiani, G. (2007). Assessment of water quality in Lake Garda (Italy) using Hyperion. *Remote Sensing of Environment,* 109 (2), 183–195, https://doi.org/10.1016/J.RSE.2006.12.017

Giardino, C., Bresciani, M., Villa, P., & Martinelli, A. (2010). Application of remote sensing in water resource management: The case study of lake Trasimeno, Italy. *Water Resources Management, 24*(14), 3885–3899. https://doi.org/10.1007/s11269-010-9639-3

Giardino, C., Pepe, M., Brivio, P. A., Ghezzi, P., & Zilioli, E. (2001). Detecting chlorophyll, Secchi disk depth and surface temperature in a sub-alpine lake using Landsat imagery. *Science of The Total Environment, 268*, 19–29. https://doi.org/10.1016/S0048-9697(00)00692-6

Gons, H. J., Auer, M. T., & Effler, S. W. (2008). MERIS satellite chlorophyll mapping of oligotrophic and eutrophic waters in the Laurentian Great Lakes. *Remote Sensing of Environment, 112*(11), 4098–4106. https://doi.org/10.1016/J.RSE.2007.06.029

Govender, M., Chetty, K., & Bulcock, H. (2007). A review of hyperspectral remote sensing and its application in vegetation and water resource studies. Water SA, 33 (2), https://doi.org/10.10520/EJC116430

Grendaitė, D., Stonevičius, E., Karosienė, J., Savadova, K., & Kasperovičienė, J. (2018). Chlorophyll-a concentration retrieval in eutrophic lakes in Lithuania from Sentinel-2 data. *Geologija. Geografija, 4*(1), 1–14. https://doi.org/10.6001/GEOL-GEOGR.V4I1.3720

Grissinger, E.H., & McDowell, L.L. (1970). Sediment in relation to water quality.*JAWRA Journal of the American Water Resources Association,* 6 (1), 7–14, https://doi.org/10.1111/J.1752-1688.1970.TB00431.X

Guimarães, T.T., Veronez, M.R., Koste, E.C., Gonzaga, L., Bordin, F., Inocencio, L.C., . . . Mauad, F.F. (2017). An alternative method of spatial autocorrelation for chlorophyll detection in water bodies using remote sensing.*Sustainability,* 9 (3), 416, https://doi.org/10.3390/SU9030416

Guimarães, T. T., Veronez, M. R., Koste, E. M., Emilie, C.and Souza, Brum, D., Gonzaga, L., & Mauad, F.F. (2019). Evaluation of regression analysis and neural networks to predict total suspended solids in water bodies from unmanned aerial vehicle images. *Sustainability, 11*(9), 2580. https://doi.org/10.3390/SU11092580

Ha, N. T. T., Koike, K., Nhuan, M. T., Canh, B. D., Thao, N. T. P., & Parsons, M. (2017). Landsat 8/OLI two bands ratio algorithm for chlorophyll-a concentration mapping in hypertrophic waters: An application to west lake in Hanoi (Vietnam). *IEEE Journal of Selected Topics in Applied Earth Observations and Remote Sensing, 10*(11), 4919–4929. https://doi.org/10.1109/JSTARS.2017.2739184

Hadjimitsis, D. G., Clayton, C. R., & Hope, V. S. (2004). An assessment of the effectiveness of atmospheric correction algorithms through the remote sensing of some reservoirs. *International Journal of Remote Sensing, 25*(18), 3651–3674. https://doi.org/10.1080/01431160310001647993

Hafeez, S., Wong, M. S., Ho, H. C., Nazeer, M., Nichol, J., Abbas, S., . . . Pun, L. (2019). Comparison of machine learning algorithms for retrieval of water quality indicators in case-II waters: A case study of Hong Kong. *Remote Sensing, 11*(6), 617. https://doi.org/10.3390/rs11060617

Harvey, E. T., Kratzer, S., & Philipson, P. (2015). Satellite-based water quality monitoring for improved spatial and temporal retrieval of chlorophyll-a in coastal waters. *Remote Sensing of Environment, 158*, 417–430. https://doi.org/10.1016/J.RSE.2014.11.017

Hashemi-Beni, L., & Gebrehiwot, A. A. (2021). Flood extent mapping: An integrated method using deep learning and region growing using UAV optical data. *IEEE Journal of Selected Topics in Applied Earth Observations and Remote Sensing, 14*,. https://doi.org/10.1109/JSTARS.2021.3051873

He, W., Chen, h., Liu, X., & Chen, J. (2008). Water quality monitoring in a slightly polluted inland water body through remote sensing-case study of the Guanting reservoir in Beijing, China. *Frontiers of Environmental Science & Engineering, 2*, 163–171. https://doi.org/10.1007/s11783-008-0027-7

Hellweger, F. L., Schlosser, P., Lall, U., & Weissel, J. K. (2004). Use of satellite imagery for water quality studies in New York harbor. *Estuarine, Coastal and Shelf Science, 61*(3), 437–448. https://doi.org/10.1016/J.ECSS.2004.06.019

Hu, C., Chen, Z., Clayton, T. D., Swarzenski, P., Brock, J. C., & Muller-Karger, F. E. (2004). Assessment of estuarine water-quality indicators using MODIS medium resolution bands: Initial results from Tampa Bay. *Remote Sensing of Environment, 93*(3), 423–441. https://doi.org/10.1016/J.RSE.2004.08.007

Hussein, N. M., & Assaf, M. N. (2020). Multispectral remote sensing utilization for monitoring chlorophyll-a levels in Inland water bodies in Jordan. *Scientific World Journal, 2020*, 1–14. https://doi.org/10.1155/2020/5060969

IOCCG (2006). Remote sensing of inherent optical properties: Fundamentals, tests of algorithms, and applications. Dartmouth, Canada.: Reports of the International Ocean-Colour Coordinating Group, No. 5, IOCCG. (Retrieved from https://doi.org/10.25607/OBP-96)

IOCCG (2018). Earth observations in support of global water quality. Dartmouth, NS, Canada: International Ocean Colour Coordinating Group (IOCCG). (Retrieved from https://doi.org/10.25607/OBP-113)

Isgró, M. A., Basallote, M. D., Caballero, I., & Barbero, L. (2022). Comparison of UAS and Sentinel-2 multispectral imagery for water quality monitoring: A case study for acid mine drainage affected areas (SW Spain). *Remote Sensing, 14*(16), 4053. https://doi.org/10.3390/RS14164053/S1

Kaba, E., Philpot, W., & Steenhuis, T. (2014). Evaluating suitability of MODIS terra images for reproducing historic sediment concentrations in water bodies: Lake Tana, Ethiopia. *International Journal of Applied Earth Observation and Geoinformation, 26*(1), 286–297. https://doi.org/10.1016/J.JAG.2013.08.001

Kabbara, N., Benkhelil, J., Awad, M., & Barale, V. (2008). Monitoring water quality in the coastal area of Tripoli (Lebanon) using high-resolution satellite data. *ISPRS Journal of Photogrammetry and Remote Sensing, 63*(5), 488–495. https://doi.org/10.1016/J.ISPRSJPRS.2008.01.004

Kabiri, K. (2023). Retrieval and validation of the Secchi disk depth values (ZSD) from the sentinel-3/OLCI satellite data in the Persian gulf and the gulf of Oman. *Environmental Science and Pollution Research, 1*, 1–13. https://doi.org/10.1007/S11356-023-27625-7

Karakoc, G., Erkoc, F. U., & Katircioglu, H. (2003). Water quality and impacts of pollution sources for Eymir and Mogan lakes (Turkey). *Environment International, 29*(1), 21–27. https://doi.org/10.1016/S0160-4120(02)00128-9

Keith, D. J., Schaeffer, B. A., Lunetta, R. S., Gould, R. W., Rocha, K., & Cobb, D. J. (2014). Remote sensing of selected water-quality indicators with the hyperspectral imager for the coastal ocean (HICO) sensor. *International Journal of Remote Sensing, 35*(9), 2927–2962. https://doi.org/10.1080/01431161.2014.894663

Keller, S., Maier, P. M., Riese, F. M., Norra, S., Holbach, A., Börsig, N., . . . Hinz, S. (2018). Hyperspectral data and machine learning for estimating CDOM, chlorophyll a, diatoms, green algae and turbidity. *International Journal of Environmental Research and Public Health, 15*(9), 1881. https://doi.org/10.3390/IJERPH15091881

Kirk, J. T. O. (1994). *Light and photosynthesis in aquatic ecosystems* (2nd ed.). Cambridge: Cambridge University Press.

Kloiber, S. M., Brezonik, P. L., Olmanson, L. G., & Bauer, M. E. (2002). A procedure for regional lake water clarity assessment using Landsat multispectral data. *Remote Sensing of Environment, 82*(1), 38–47. https://doi.org/10.1016/S0034-4257(02)00022-6

Knight, J. F., & Voth, M. L. (2012). Application of MODIS imagery for intra-annual water clarity assessment of Minnesota lakes. *Remote Sensing, 4*(7), 2181–2198. https://doi.org/10.3390/RS4072181

Kutser, T. (2004). Quantitative detection of chlorophyll in cyanobacterial blooms by satellite remote sensing. *Limnology and Oceanography, 49*(6), 2179–2189. https://doi.org/10.4319/LO.2004.49.6.2179

Kutser, T. (2012). The possibility of using the Landsat image archive for monitoring long time trends in coloured dissolved organic matter concentration in lake waters. *Remote Sensing of Environment, 123*, 334–338. https://doi.org/10.1016/J.RSE.2012.04.004

Kutser, T., Paavel, B., Verpoorter, C., Ligi, M., Soomets, T., Toming, K., & Casal, G. (2016). Remote sensing of black lakes and using 810 nm reflectance peak for retrieving water quality parameters of optically complex waters. *Remote Sensing, 8*(6), 497. https://doi.org/10.3390/RS8060497

Kutser, T., Pierson, D. C., Kallio, K. Y., Reinart, A., & Sobek, S. (2005). Mapping lake CDOM by satellite remote sensing. *Remote Sensing of Environment, 94*, 535–540. https://doi.org/10.1016/J.RSE.2004.11.009

Lai, Y., Zhang, J., Song, Y., & Gong, Z. (2021). Retrieval and evaluation of chlorophyll-a concentration in reservoirs with main water supply function in Beijing, China, based on Landsat satellite images. *International Journal of Environmental Research and Public Health, 18*(9), 4419. https://doi.org/10.3390/ijerph18094419

Lee, Z., Marra, J., Perry, M. J., & Kahru, M. (2015). Estimating oceanic primary productivity from ocean color remote sensing: A strategic assessment. *Journal of Marine Systems, 149*, 50–59. https://doi.org/10.1016/J.JMARSYS.2014.11.015

Li, S., Song, K., Mu, G., Zhao, Y., Ma, J., & Ren, J. (2016). Evaluation of the quasi- analytical algorithm (QAA) for estimating total absorption coefficient of turbid inland waters in Northeast China. *IEEE Journal of Selected Topics in Applied Earth Observations and Remote Sensing, 9*(9), 4022–4036. https://doi.org/10.1109/JSTARS.2016.2549026

Lin, J., Lyu, H., Miao, S., Pan, Y., Wu, Z., Li, Y., & Wang, Q. (2018). A two step approach to mapping particulate organic carbon (POC) in Inland water using OLCI images. *Ecological Indicators, 90*, 502–512. https://doi.org/10.1016/J.ECOLIND.2018.03.044

Liu, G., Li, Y., Lyu, H., Wang, S., Du, C., & Huang, C. (2016). An improved land target-based atmospheric correction method for lake Taihu. *IEEE Journal of Selected Topics in Applied Earth Observations and Remote Sensing, 9*(2), 793–803. https://doi.org/10.1109/JSTARS.2015.2503800

Lu, Q., Si, W., Wei, L., Li, Z., Xia, Z., Ye, S., & Xia, Y. (2021). Retrieval of water quality from UAV-borne hyperspectral imagery: A comparative study of machine learning algorithms. *Remote Sensing*, 13 (19), 3928, https://doi.org/10.3390/RS13193928

Lu, S., Ouyang, N., Wu, B., Wei, Y., & Tesemma, Z. (2013). Lake water volume calculation with time series remote-sensing images. *International Journal of Remote Sensing, 34*(22), 7962–7973. https://doi.org/10.1080/01431161.2013.827814

Ma, R., & Dai, J. (2007). Investigation of chlorophyll-a and total suspended matter concentrations using Landsat ETM and field spectral measurement in Taihu lake. *China. International Journal of Remote Sensing, 26*(13), 2779–2795. https://doi.org/10.1080/01431160512331326648

Maciel, D. A., Barbosa, C. C. F., Novo, E.M.L.d.M., Júnior, R.F., & Begliomini, F.N. (2021). Water clarity in Brazilian water assessed using Sentinel-2 and machine learning methods. *ISPRS Journal of Photogrammetry and Remote Sensing, 182*, 134–152. https://doi.org/10.1016/J.ISPRSJPRS.2021.10.009

Markogianni, V., Kalivas, D., Petropoulos, e.P., & Dimitriou, E. (2020). Estimating chlorophyll-a of Inland water bodies in Greece based on Landsat data. *Remote Sensing, 12*(13), 2087. https://doi.org/10.3390/RS12132087

Martins, V. S., Barbosa, C. C. F., De Carvalho, L. A. S., Jorge, D. S. F., Lobo, F. D. L., & Novo, E. M. L. D. M. (2017). Assessment of atmospheric correction methods for Sentinel-2 MSI images applied to Amazon floodplain lakes. *Remote Sensing, 9*(4), 322. https://doi.org/10.3390/RS9040322

Matthews, M. W. (2011). A current review of empirical procedures of remote sensing in inland and near-coastal transitional waters. *International Journal of Remote Senisng, 32*(21), 6855–6899. https://doi.org/10.1080/01431161.2010.512947

Matthews, M. W., Bernard, S., & Winter, K. (2010). Remote sensing of cyanobacteria dominant algal blooms and water quality parameters in Zeekoevlei, a small hypertrophic lake, using MERIS. *Remote Sensing of Environment, 114*(9), 2070–2087. https://doi.org/10.1016/J.RSE.2010.04.013

Mbuh, M. (2019). Use of hyperspectral remote sensing to estimate water quality. J. Chen, Y. Song, & H. Li (Eds.), *Processing and analysis of hyperspectral data* (p. 107–124). Rijeka: IntechOpen.

McCullough, I. M., Loftin, C. S., & Sader, tA. (2012). High-frequency remote monitoring of large lakes with MODIS 500m imagery. *Remote Sensing of Environment, 124*, 234–241. https://doi.org/10.1016/J.RSE.2012.05.018

Mishra, S., Mishra, D. R., & Lee, Z. (2014). Bio-optical inversion in highly turbid and cyanobacteria-dominated waters. *IEEE Transactions on Geoscience and Remote Sensing, 52*(1), 375–388. https://doi.org/10.1109/TGRS.2013.2240462

Mobley, C.D., Werdell, J., Franz, B., Ahmad, Z.,& Bailey, S. (2016). *Atmospheric correction for satellite ocean color radiometry.* (Rretrieved from https://oceancolor.gsfc.nasa.gov/docs/technical/NASA-TM-2016-217551.pdf)

Morel, A., & Prieur, L. (1977). Analysis of variations in ocean color. *Limnology and Oceanography, 22*(4), 709–722. https://doi.org/10.4319/LO.1977.22.4.0709

Moses, W. J., Bowles, J. H., & Corson, M. R. (2015). Expected improvements in the quantitative remote sensing of optically complex waters with the use of an optically fast hyperspectral spectrometer—A modeling study. *Sensors, 15*(3), 6152–6173. https://doi.org/10.3390/S150306152

Moses, W. J., Gitelson, A. A., Berdnikov, S., & Povazhnyy, V. (2009). Satellite estimation of chlorophyll-a concentration using the red and NIR bands of MERISThe azov sea case study. *IEEE Geoscience and Remote Sensing Letters, 6*(4), 845–849. https://doi.org/10.1109/LGRS.2009.2026657

Moses, W. J., Sterckx, S., Montes, M. J., De Keukelaere, L., & Knaeps, E. (2017). Atmospheric correction for inland waters. *Bio-optical Modeling and Remote Sensing of Inland Waters, 69–100*,. https://doi.org/10.1016/B978-0-12-804644-9.00003-3

Murugan, P., Sivakumar, R., Pandiyan, R., & Annadurai, M. (2016). Comparison of in-situ hyperspectral and Landsat ETM+ data for chlorophyll-a mapping in case II water (Krishnarajapuram Lake, Bangalore). *Journal of the Indian Society of Remote Sensing, 44*(6), 949–957. https://doi.org/10.1007/S12524-015-0531-8

Muscutt, A. D., Harris, G. L., Bailey, S. W., & Davies, D. B. (1993). Buffer zones to improve water quality: A review of their potential use in UK agriculture. *Agri culture, Ecosystems & Environment, 45*(1–2), 59–77. https://doi.org/10.1016/0167-8809(93)90059-X

Nas, B., Ekercin, S., Karabörk, H., Berktay, A., & Mulla, D. J. (2010). An application of Landsat-5TM image data for water quality mapping in lake Beysehir, Turkey. *Water, Air, and Soil Pollution, 212*(1–4), 183–197. https://doi.org/10.1007/S11270-010-0331-2

Nas, B., Karabork, H., Ekercin, S., & Berktay, A. (2009). Mapping chlorophyll-a through in-situ measurements and Terra ASTER satellite data. *Environmental Monitoring and Assessment, 157*, 375–382. https://doi.org/10.1007/S10661-008-0542-9

Niroumand-Jadidi, M., Bovolo, F., & Bruzzone, L. (2020). Water quality retrieval from PRISMA hyperspectral images: First experience in a turbid lake and comparison with Sentinel-2. *Remote Sensing, 12*(23), 3984. https://doi.org/10.3390/RS12233984

Ogashawara, I., Li, L., & Druschel, G.K. (2022). Retrieval of inherent optical properties from multiple aquatic systems using a quasi-analytical algorithm for several water types. *Remote Sensing Applications: Society and Environment,* 27, 100807, https://doi.org/10.1016/j.rsase.2022.100807

Olivetti, D., Roig, H., Martinez, J. M., Borges, H., Ferreira, A., Casari, R., . . . Malta, E. (2020). Low-cost unmanned aerial multispectral imagery for siltation monitoring in reservoirs. *Remote Sensing, 12*(11), 1855. https://doi.org/10.3390/RS12111855

Osibanjo, O., Daso, A. P., & Gbadebo, A. M. (2013). The impact of industries on surface water quality of River Ona and River Alaro in Oluyole Industrial Estate, Ibadan, Nigeria. *African*

Journal of Biotechnology, 10(4), 696–702. https://doi.org/10.4314/ajb.v10i4

Oyama, Y., Matsushita, u., Fukushima, T., Matsushige, K., & Imai, A. (2009). Application of spectral decomposition algorithm for mapping water quality in a turbid lake (Lake Kasumigaura, Japan) from Landsat tm data. *ISPRS Journal of Photogrammetry and Remote Sensing, 64*(1), 73–85. https://doi.org/10.1016/J.ISPRSJPRS.2008.04.005

Östlund, C., Flink, P., Strömbeck, N., Pierson, D., & Lindell, T. (2001). Mapping of the water quality of lake Erken, Sweden, from imaging spectrometry and land sat thematic mapper. *Science of The Total Environment, 268*(1–3), 139–154. https://doi.org/10.1016/S0048-9697(00)00683-5

Page, B. P., Olmanson, L. G., & Mishra, D. R. (2019). A harmonized image processing workflow using Sentinel-2/MSI and Landsat-8/OLI for mapping water clarity in optically variable lake systems. *Remote Sensing of Environment, 231*,. https://doi.org/10.1016/J.RSE.2019.111284

Pahlevan, N., Mangin, A., Balasubramanian, S.V., Smith, B., Alikas, K., Arai, K., . . . Warren, M. (2021). ACIX-Aqua: A global assessment of atmospheric correction methods for Landsat-8 and Sentinel-2 over lakes, rivers, and coastal waters.*Remote Sensing of Environment,* 258 , 112366, https://doi.org/10.1016/J.RSE.2021.112366

Pahlevan, N., Smith, B., Binding, C., Gurlin, D., Li, L., Bresciani, M., & Giardino, C. (2021). Hyperspectral retrievals of phytoplankton absorption and chlorophyll-a in inland and nearshore coastal waters. *Remote Sensing of Environment, 253*, 12200. https://doi.org/10.1016/J.RSE.2020.112200

Pahlevan, N., Smith, B., Schalles, J., Binding, C., Cao, Z., Ma, R., . . . Stumpf, R. (2020). Seamless retrievals of chlorophyll-a from Sentinel-2 (MSI) and Sentinel- 3 (OLCI) in inland and coastal waters: A machine-learning approach. *Remote Sensing of Environment, 240*, 111604. https://doi.org/10.1016/J.RSE.2019.111604

Palmer, S. C., Kutser, T., & Hunter, P. D. (2015). Remote sensing of inland waters: Challenges, progress and future directions. *Remote Sensing of Environment, 157*, 1–8. https://doi.org/10.1016/J.RSE.2014.09.021

Petch, J., Di, S., & Nelson, W. (2022). Opening the black box: The promise and limitations of explainable machine learning in cardiology. *Canadian Journal of Cardiology, 38*(2), 204–213. https://doi.org/10.1016/J.CJCA.2021.09.004

Peterson, K. T., Sagan, V., & Sloan, J. J. (2020). Deep learning-based water quality estimation and anomaly detection using Landsat-8/Sentinel-2 virtual constellation and cloud computing. *GIScience & Remote Sensing, 57*(4), 510–525. https://doi.org/10.1080/15481603.2020.1738061

Philipson, P., Kratzer, S., Mustapha, S. B., Strömbeck, N., & Stelzer, K. (2016). Satellite based water quality monitoring in lake Vänern, Sweden. *International Journal of Remote Sensing, 37*(16), 3938–3960. https://doi.org/10.1080/01431161.2016.1204480

Qin, Y., Brando, V.E., Dekker, A.G., & Blondeau-Patissier, D. (2007). Validity of SeaDAS water constituents retrieval algorithms in Australian tropical coastal waters. *Geo- physical Research Letters,* 34 (21), https://doi.org/10.1029/2007GL030599

Rahul, T. S., Brema, J., & Wessley, G. J. J. (2023). Evaluation of surface water quality of Ukkadam Lake in Coimbatore using UAV and Sentinel-2 multispectral data. *Inter national Journal of Environmental Science and Technology, 20*(3), 3205–3220. https://doi.org/10.1007/s13762-022-04029-7

Rodrigues, T., Alcântara, E., Watanabe, F., & Imai, N. (2017). Retrieval of Secchi disk depth from a reservoir using a semi-analytical scheme. *Remote Sensing of Environment, 198*, 213–228. https://doi.org/10.1016/J.RSE.2017.06.018

Rostom, N. G., Shalaby, A. A., Issa, Y. M., & Afifi, A. A. (2017). Evaluation of Mariut Lake water quality using hyperspectral remote sensing and laboratory works. *The Egyptian Journal of Remote Sensing and Space Science, 20*, S39–S48. https://doi.org/10.1016/J.EJRS.2016.11.002

Rubin, H. J., Lutz, D. A., Steele, B. G., Cottingham, K. L., Weathers, K. C., Ducey, M. J., . . . Chipman, J. W. (2021). Remote sensing of lake water clarity: Performance and transferability of both historical algorithms and machine learning. *Remote Sensing, 13*(8), 1434. https://doi.org/10.3390/RS13081434

Saberioon, M., Brom, J., Nedbal, V., & Souček, P., & Cisař, P. (2020). Chlorophyll-a and total suspended solids retrieval and mapping using Sentinel-2a and machine learning for inland waters. *Ecological Indicators, 113*,. https://doi.org/10.1016/J.ECOLIND.2020.106236

Sagan, V., Peterson, K. T., Maimaitijiang, M., Sidike, P., Sloan, J., Greeling, B. A., . . . Adams, C. (2020). Monitoring inland water quality using remote sensing: Potential and limitations of spectral indices, bio-optical simulations, machine learning, and cloud computing. *Earth-Science Reviews, 205*, 103187. https://doi.org/10.1016/J.EARSCIREV.2020.103187

Sawaya, K. E., Olmanson, L. G., Heinert, N. J., Brezonik, a.L., & Bauer, a.E. (2003). Extending satellite remote sensing to local scales: Land and water resource monitoring using high-resolution imagery. *Remote Sensing of Environment, 88*, 144–156. https://doi.org/10.1016/J.RSE.2003.04.006

Sayers, M. J., Grimm, A. G., Shuchman, R. A., Deines, A. M., Bunnell, D. B., Raymer, Z. B., . . . Mychek-Londer, J. (2015). A new method to generate a high-resolution global distribution map of lake chlorophyll. *International Journal of Remote Sensing, 36*(7), 1942–1964. https://doi.org/10.1080/01431161.2015.1029099

Shen, M., Duan, H., Cao, Z., Xue, K., Qi, T., Ma, J., . . . Song, X. (2020). Sentinel-3 OLCI observations of water clarity in large lakes in Eastern China: Implications for SDG 6.3.2 evaluation. *Remote Sensing of Environment, 247*, 111950, https://doi.org/10.1016/J.RSE.2020.111950

Shi, W., & Wang, M. (2019). A blended inherent optical property algorithm for global satellite ocean color observations. *Limnology and Oceanography: Methods,* 17 (7), 377–394, https://doi.org/10.1002/lom3.10320

Simis, S. G., Peters, S. W., & Gons, H. J. (2005). Remote sensing of the cyanobacterial pigment phycocyanin in turbid inland water. *Limnology and Oceanography, 50*(1), 237–245. https://doi.org/10.4319/LO.2005.50.1.0237

Skarbøvik, E., & Roseth, R. (2014). Use of sensor data for turbidity, pH and conductivity as an alternative to conventional water quality monitoring in four Norwegian case studies. *Acta Agriculturae Scandinavica, Section B - Soil & Plant Science, 65*(1), 63–73. https://doi.org/10.1080/09064710.2014.966751

Soriano-González, J., Urrego, E. P., Sòria-Perpinyà, X., Angelats, E., Alcaraz, C., Delegido, J., . . . Moreno, J.

(2022). Towards the combination of C2RCC processors for improving water quality retrieval in inland and coastal areas. *Remote Sensing, 14*(5), 1124. https://doi.org/10.3390/RS14051124

Su, P. W., & Lo, S. L. (2022). Satellite imagery: A way to monitor water quality for the future? *Environmental Science and Pollution Research, 29*(38), 57022–57029. https://doi.org/10.1007/S11356-022-21524-Z

Su, T.-C., Chou, H.-T., Martinsanz, G. P., Müller, R., Lucieer, A., & Thenkabail, P. S. (2015). Application of multispectral sensors carried on unmanned aerial vehicle (UAV) to trophic state mapping of small reservoirs: A case study of Tain-Pu reservoir in Kinmen. *Taiwan. Remote Sensing, 7*(8), 10078–10097. https://doi.org/10.3390/RS70810078

Sudheer, K. P., Chaubey, I., & Garg, V. (2006). Lake water quality assessment from land sat thematic mapper data using neural network: An approach to optimal band combination selection. *JAWRA Journal of the American Water Resources Association, 42*, 1683–1695. https://doi.org/10.1111/J.1752-1688.2006.TB06029.X

Sun, F., Sun, W., Chen, J., & Gong, P. (2012). Comparison and improvement of methods for identifying waterbodies in remotely sensed imagery. *International Journal of Remote Sensing, 33*(21), 6854–6875. https://doi.org/10.1080/01431161.2012.692829

Tan, J., Cherkauer, K. A., & Chaubey, I. (2011). Using hyperspectral data to quantify water-quality parameters in the Wabash River and its tributaries. *Indiana. International Journal of Remote Sensing, 36*(21), 5466–5484. https://doi.org/10.1080/01431161.2015.1101654

Tarrant, P. E., Amacher, J. A., & Neuer, S. (2010). Assessing the potential of medium-resolution imaging spectrometer (MERIS) and moderate-resolution imaging spectroradiometer (MODIS) data for monitoring total suspended matter in small and intermediate sized lakes and reservoirs. *Water Resources Research, 46*(9), 9532. https://doi.org/10.1029/2009WR008709

Tebbs, E. J., Remedios, J. J., & Harper, D. M. (2013). Remote sensing of chlorophyll a as a measure of cyanobacterial biomass in lake Bogoria, a hypertrophic, saline–alkaline, Amingo lake, using Landsat ETM+. *Remote Sensing of Environment, 135*, 92–106. https://doi.org/10.1016/J.RSE.2013.03.024

Tian, S., Guo, H., Xu, W., Zhu, X., Wang, B., Zeng, Q., . . . Huang, J. J. (2023). Remote sensing retrieval of inland water quality parameters using Sentinel-2 and multiple machine learning algorithms. *Environmental Science and Pollution Research, 30*(7), 18617–18630. https://doi.org/10.1007/s11356-022-23431-9

Toming, K., Kutser, T., Laas, A., Sepp, M., Paavel, B., & Nõges, T. (2016). First experiences in mapping lake water quality parameters with Sentinel-2 MSI imagery. *Remote Sensing 2016, vol. 8, Page 640,* 8 (8), 640, https://doi.org/10.3390/RS8080640

Topp, S.N., Pavelsky, T.M., Jensen, D., Simard, M., & Ross, M.R. (2020). Research trends in the use of remote sensing for inland water quality science: Moving towards multidisciplinary applications. *Water 2020, vol. 12, Page 169 , 12*(1), 169, https://doi.org/10.3390/W12010169

Tyler, A. N., Svab, E., Preston, T., Présing, M., & Kovács, W. A. (2006). Remote sensing of the water quality of shallow lakes: A mixture modelling approach to quantifying phytoplankton in water characterized by high-suspended sediment. *International Journal of Remote Sensing, 27*(8), 1521–1537. https://doi.org/10.1080/01431160500419311

United Nations (2022). The sustainable development goals report 2022. (Retrieved from https://unstats.un.org/sdgs/report/2022/The-Sustainable-Development-Goals-Report-2022.pdf)

United Nations Environment Programme (2021). Progress on ambient water quality: Tracking SDG 6 series: Global indicator 6.3.2 updates and acceleration needs. (Retrieved from https://www.unwater.org/sites/default/les/app/uploads/2021/09/SDG6_Indicator_Report_632_Progress-on-Ambient-Water-Quality_2021_EN.pdf)

Vermote, E. F., Tanré, D., Deuzé, e.L., Herman, M., & Morcrette, J.J. (1997). Second simulation of the satellite signal in the solar spectrum, 6s: An overview. *IEEE Transactions on Geoscience and Remote Sensing, 35*(3), 675–686. https://doi.org/10.1109/36.581987

Wang, D., Ma, R., Xue, K., & Loiselle, S. A. (2019). The assessment of Landsat-8 OLI atmospheric correction algorithms for inland waters. *Remote Sensing, 11*(2), 169. https://doi.org/10.3390/RS11020169

Wang, Q., Song, K., Xiao, X., Jacinthe, P. A., Wen, Z., Zhao, F., . . . Liu, G. (2022). Mapping water clarity in North American lakes and reservoirs using Landsat images on the GEE platform with the RGRB model. *ISPRS Journal of Photogram metry and Remote Sensing, 194*, 39–57. https://doi.org/10.1016/J.ISPRSJPRS.2022.09.014

Watanabe, F. S. Y., Alcântara, E., Rodrigues, T. W. P., Imai, N. N., Barbosa, C. C. F., & Rotta, LHd. S. (2015). Estimation of chlorophyll-a concentration and the trophic state of the Barra Bonita hydroelectric reservoir using OLI/Landsat-8 images. *International Journal of Environmental Research and Public Health, 12*(9), 10391–10417. https://doi.org/10.3390/IJERPH120910391

Welcomme, R.L. (2011). An overview of global catch statistics for inland fish. *ICES Journal of Marine Science,* 68 (8), , https://doi.org/10.1093/ICESJMS/FSR035

Wen, X.-P., & Yang, X.-F. (2011). Monitoring of water quality using remote sensing data mining. K. Funatsu (Ed.), Knowledge-oriented applications in data mining (p. 135–145). Rijeka: IntechOpen.

Werdell, P. J., Franz, B. A., & Bailey, S. W. (2010). Evaluation of shortwave infrared atmospheric correction for ocean color remote sensing of Chesapeake Bay. *Remote Sensing of Environment, 114*(10), 2238–2247. https://doi.org/10.1016/J.RSE.2010.04.027

Werdell, P. J., Franz, B. A., Bailey, S. W., Feldman, G. C., Boss, E., Brando, V. E., . . . Mangin, A. (2013). Generalized ocean color inversion model for retrieving marine inherent optical properties. *Applied Optics, 52*(10), 2019–2037. https://doi.org/10.1364/AO.52.002019

Wu, J. L., Ho, C. R., Huang, C. C., Srivastav, A. L., Tzeng, J. H., & Lin, Y. T. (2014). Hyperspectral sensing for turbid water quality monitoring in freshwater rivers: Empirical relationship between reflectance and turbidity and total solids. *Sensors, 14*(12), 22670–22688. https://doi.org/10.3390/S141222670

Xiao, Y., Guo, Y., Yin, G., Zhang, X., Shi, Y., Hao, F., & Fu, Y. (2022). UAV multispectral image-based urban river

water quality monitoring using stacked ensemble machine learning algorithms: A case study of the Zhanghe River, China. *Remote Sensing, 14*(14), 3272. https://doi.org/10.3390/rs14143272
Yan, W. Y., Shaker, A., & El-Ashmawy, N. (2015). Urban land cover classification using airborne lidar data: A review. *Remote Sensing of Environment, 158*, 295–310. https://doi.org/10.1016/J.RSE.2014.11.001
Yan, Y., Wang, Y., Yu, C., & Zhang, Z. (2023). Multispectral remote sensing for estimating water quality parameters: A comparative study of inversion methods using unmanned aerial vehicles (UAVs). *Sustainability, 15*(13), 10298. https://doi.org/10.3390/su151310298
Yang, H., Kong, J., Hu, H., Du, Y., Gao, M., & Chen, F. (2022). A review of remote sensing for water quality retrieval: Progress and challenges. *Remote Sensing 2022, 14* (8), 1770, https://doi.org/10.3390/RS14081770
Yang, W., Matsushita, B., Chen, J., & Fukushima, T. (2011). Estimating constituent concentrations in case II waters from MERIS satellite data by semi-analytical model optimizing and look-up tables. *Remote Sensing of Environment, 115*(5), 1247–1259. https://doi.org/10.1016/J.RSE.2011.01.007
Yang, Z., Gong, C., Ji, T., Hu, Y., & Li, L. (2022). Water quality retrieval from zy1-02d hyperspectral imagery in urban water bodies and comparison with Sentinel-2. *Remote Sensing 2022, Vol. 14, Page 5029,* 14 (19), 5029, https://doi.org/10.3390/RS14195029
Yen, H., Hoque, Y., Harmel, R. D., & Jeong, J. (2015). The impact of considering uncertainty in measured calibration/validation data during auto-calibration of hydrologic and water quality models. *Stochastic Environmental Research and Risk Assessment, 29*(7), 1891–1901. https://doi.org/10.1007/S00477-015-1047-Z
Yulong, G., Changchun, H., Yunmei, L., Chenggong, D., Lingfei, S., Yuan, L., . . . Guangxing, J. (2022). Hyperspectral reconstruction method for optically complex inland waters based on bio-optical model and sparse representing. *Remote Sensing of Environment, 276*, 113045. https://doi.org/10.1016/J.RSE.2022.113045
Zang, W., Lin, J., Wang, Y., & Tao, H. (2012). Investigating small-scale water pollution with UAV remote sensing technology. *World automation congress 2012* (p. 1-4).
Zeng, C., Richardson, M., & King, D. J. (2017). The impacts of environmental variables on water reflectance measured using a lightweight unmanned aerial vehicle (UAV)- based spectrometer system. *ISPRS Journal of Photogrammetry and Remote Sensing, 130*, 217–230. https://doi.org/10.1016/J.ISPRSJPRS.2017.06.004
Zhang, J., Fu, P., Meng, F., Yang, X., Xu, J., & Cui, Y. (2022). Estimation algorithm for chlorophyll-a concentrations in water from hyperspectral images based on feature derivation and ensemble learning. *Ecological Informatics, 71*, 101783. https://doi.org/10.1016/J.ECOINF.2022.101783
Zhang, Y., Guo, F., Meng, W., & Wang, X.-Q. (2008). Water quality assessment and source identification of Daliao River basin using multivariate statistical methods. *Environmental Monitoring and Assessment 2008 152:1,* 152 (1), 105–121, https://doi.org/10.1007/S10661-008-0300-Z
Zhang, Y., Kong, X., Deng, L., & Liu, Y. (2023). Monitor water quality through retrieving water quality parameters from hyperspectral images using graph convolution network with superposition of multi-point effect: A case study in Maozhou River. *Journal of Environmental Management, 342*, 118283, https://doi.org/10.1016/J.JENVMAN.2023.118283
Zhang, Y., Wu, L., Deng, L., & Ouyang, B. (2021). Retrieval of water quality parameters from hyperspectral images using a hybrid feedback deep factorization machine model. *Water Research, 204*, 117618. https://doi.org/10.1016/J.WATRES.2021.117618
Zhang, Y., Wu, L., Ren, H., Liu, Y., Zheng, Y., Liu, Y., & Dong, J. (2020). Mapping water quality parameters in urban rivers from hyperspectral images using a new self-adapting selection of multiple artificial neural networks. *Remote Sensing, 12*(2), 336. https://doi.org/10.3390/RS12020336
Zhong, Y., Wang, X., Wang, S., & Zhang, L. (2021). Advances in spaceborne hyperspectral remote sensing in China. *Geo-spatial Information Science, 24*(1), 95–120. https://doi.org/10.1080/10095020.2020.1860653
Zhou, W., Wang, S., Zhou, Y., & Troy, A. (2008). Mapping the concentrations of total suspended matter in lake Taihu, China, using Landsat-5 TM data. *International Journal of Remote Sensing, 27*(6), 1177–1191. https://doi.org/10.1080/01431160500353825